[redacted]

Development and Evaluation of Contaminant Removal Technologies for Landfill Gas Processing

Date of Submission (03/2017)

John N. Kuhn

University of South Florida

Department of Chemical & Biomedical Engineering

Babu Joseph

University of South Florida

Department of Chemical & Biomedical Engineering

Hinkley Center for Solid and Hazardous Waste Management

University of Florida

P. O. Box 116016

Gainesville, FL 32611

www.hinkleycenter.org

Report #

Acknowledgments

The authors gratefully acknowledge funding from Hinkley Center for Solid and Hazardous Waste Management, the Graduate Students Success Fellowship (to NHE) that is administered by the USF School of Graduate Studies, and the NASA Dissertation Completion Fellowship that is administered by the Florida Space Grant Consortium.

TABLE OF CONTENTS

List of Figures

List of Tables

List of Abbreviations, Acronyms and Units of Measurements

i.	Dry reforming of methane:	DRM
ii.	Fischer Tropsch Synthesis:	FTS
iii.	Water gas Shift:	WGS
iv.	Reverse water gas shift:	rWGS
v.	Greenhouse Gas:	GHG
vi.	Landfill Gas:	LFG
vii.	Environmental Protection Agency:	EPA
viii.	Oxygen Storage Capacity:	OSC
ix.	Temperature Programmed Reduction:	TPR
x.	Temperature Programmed Desorption-CO_2:	TPD
xi.	Temperature Programmed Oxidation:	TPO
xii.	Temperature Programmed Reactions:	TP-rxns
xiii.	X-ray Diffraction:	XRD
xiv.	Mass spectrometer:	MS
xv.	Wetness Impregnation:	WI
xvi.	Gas hourly space velocity:	GHSV
xvii.	Turnover frequency:	TOF
xviii.	Time-on-stream:	TOS
xix.	Brunauer, Emmett and Teller:	BET
xx.	Barrett Joyner Halenda:	BJH
xxi.	Volatile Methyl Siloxanes:	VMS

ABSTRACT

Regardless of whether landfill gas (LFG) is being flared or converted to energy (electricity, compressed natural gas, or liquid hydrocarbon fuels), contaminant issues must be addressed to minimize emissions and increase equipment lifetimes. The common contaminants include halides, sulfides, as well as volatile methyl siloxanes (VMS) and the economical and environmentally sound removal of these contaminants is an increasingly pressing issue. Catalytic reforming of landfill gas has been suggested to help produce synthesis gas (H_2 and CO) which can be used as a feedstock for Fischer Tropsch Synthesis (FTS) to obtain valuable liquid hydrocarbon fuels. However prior to reforming, the poisoning effect of VMSs must be determined. This research effort will address the poisoning effect of decomposed siloxanes over both high and low temperature catalysts and model the effects of relative humidity and bed height using COMSOL® Multiphysics with activated carbon as the adsorbent.

To accomplish these goals, the effect of siloxanes were simulated by coating both the high and low temperature dry reforming catalyst particles with silica, which is the decomposition product of siloxanes. The high temperature dry reforming catalyst particles were comprised of 1.3 wt%Ni-1.0 wt% Mg on a ceria zirconia oxide support and the low temperature reforming catalyst composed of 0.16 wt% Pt-1.3 wt% Ni-1.0 wt% Mg on the same support. The catalysts were poisoned using three different levels, simulating equivalents of 1 week, 1 month, and 6 months of poisoning. Temperature-programmed reduction studies for the 0.16Pt doped catalyst showed that the temperature of the reduction feature increased significantly at even the smallest poisoning level (1 week equivalent); increasing from 248 to 304 °C which is an indication of catalyst deactivation. The reduction temperature continued to increase with extended silica poisoning, reaching 311 °C at 1 month of poisoning and 315 °C at 6 months of poisoning. Characterization studies on the poisoned catalysts showed the presence of crystalline (XRD and FT-IR) and amorphous (FT-IR) silica species that were not found in the fresh catalyst. Dry reforming experiments showed that poisoning has adversely affected the catalysts by increasing the temperature at which both 10% (X_{10}) and 50% (X_{50}) conversion of both CH_4 as well as CO_2 occurs. Methane X_{10} increased from 454°C for the fresh catalyst to 518 °C for 1week poisoning and reached 587 °C for 6 months of poisoning in the 0.16Pt doped catalyst. Similarly the NiMg-only catalyst had an increase in methane X_{10} from 762 °C for the fresh catalyst to 810 °C at 1 week poisoning reaching 842 °C at

1 month poisoning and never reaching X_{10} for 6 months of poisoning, indicating severe deactivation of the catalyst. Overall, the results of this study indicate substantial Si species removal is required for catalytic conversion of LFG. The simulation portion of the study was done to simulate a comprehensive model for a full-scale process using current LFG purification technologies. COMSOL® Multiphysics version 5.2 was utilized for the simulation. The model was used to appropriately size and cost the LFG purification process. In order to account for the different LFG-to-energy projects, a model was developed for three common LFG applications: direct use (engines), electricity generation (fuel cells), and conversion to liquid hydrocarbon fuels (catalysis). Each process was designed to have a minimum adsorption bed life of 6 months and optimized for moisture content to design an appropriate pre-treatment step. Overall, it was determined that in order to keep the VMS adsorption appreciable, the maximum allowable moisture content of LFG before purification should be 50% relative humidity at STP. These two conditions along with the average LFG flow (2500 SCFM) and a high-end level of VMS (15 mg/m^3) gave the required adsorption bed heights of 10 feet for engine applications, 20 feet for catalysts applications, and 30 feet for fuel cell applications. The cost of each of these processes was determined with the inclusion of H_2S removal, and costs were compared with that of VMS removal. The annual costs for impurity removal in the three applications are $1.16E6 (engines), $1.19E6 (fuel cells), and $1.22E6 (catalysis). This corresponds to $31.8, $32.6, and $33.3 per kilogram of contaminant removed and $0.031, $0.032, and $0.033 per Nm^3 of LFG processed respectively. H_2S removal accounts for roughly 2/3 of the yearly cost of the three LFG clean up processes.

1. INTRODUCTION AND BACKGROUND

Alternative fuel sources are no longer optional, but are now a necessity as a result of increasing energy demands and declining fossil fuel reserves. Waste-to-energy projects are an increasingly prominent component of future energy portfolios. Landfill gas (LFG)-to-energy projects are particularly important as they address greenhouse gas emissions. Catalytic dry reforming of methane (DRM) has been extensively studied in recent years as it can produce H_2 and CO (Baudouin *et al* 2014, Bradford and Vannice 1999, Damyanova *et al* 2009a, Damyanova *et al* 2009b, Elsayed *et al* 2016, Elsayed *et al* 2015, Pakhare and Spivey 2014, Rostrup-Nielsen *et al* 2002, Yamaguchi and Iglesia 2010, Zhang and Verykios 1996, Zhang and Verykios 1995). Reforming of biomass derived biogas can produce a H_2:CO ratio of 2:1 which is ideal for Fischer Tropsch Synthesis (FTS) to produce high value liquid hydrocarbon fuels, and methanol synthesis, when combined with other reactions such as steam reforming (Bradford and Vannice 1999, Song and Pan 2004) or the water-gas shift (WGS). However, contaminants in LFG may hamper these projects both from environmental and economic standpoints.

The goal of this research effort is to determine the effect of select contaminants (siloxanes) on the reforming catalyst and evaluate cleanup technologies to determine the most efficient and cost effective method for gas cleanup. To accomplish these goals, both experimental work as well as modeling were done along with extensive literature review. Two catalyst systems, a low temperature one (comprised of 0.16wt%Pt-1.3wt%Ni-1.0wt%Mg/$Ce_{0.6}Zr_{0.4}O_2$) and a high temperature one (comprised of 1.3wt%Ni-1.0wt%Mg/$Ce_{0.6}Zr_{0.4}O_2$) were poisoned using three amounts of decomposed siloxanes equivalent to 1 week, 1 month and 6 months of poison. The catalysts were extensively characterized and model biogas was flown over them to determine the effect of poisoning on the catalytic activity and conversion temperature. COMSOL® Multiphysics was used to model the separation of volatile methyl siloxanes (VMS) contaminants from landfill gas using fixed adsorption beds with the objective of identifying the most appropriate technology and the economics associated with the purification step. A parametric sweep was done to test 162 unique cases in which the varied parameters were: adsorbent type, bed height, inlet VMS concentration, moisture content, and VMS limit. Three different energy conversion technologies were explored: direct conversion to electricity using IC engines, conversion to liquid hydrocarbon fuels using catalytic conversion, and electricity generation using fuel cells. The appropriate size and conditions for each conversion process were determined with the goal of meeting a minimum breakthrough time of 6 months (180 days). Overall results, discussions and conclusions from the experimental as well as modeling work are presented in the next sections of this report.

1.1 Biomass

Biomass, the carbon based byproduct of the anaerobic digestion of living or deceased organisms and materials, produces biogas (CH_4 and CO_2) through several pathways. Biomass can come from industrial residues, animal wastes, municipal solid waste (MSW), sludge digesters and agricultural crops.

Biomass also possesses the attractive quality of being a carbon neutral energy source since the carbon dioxide produced is largely the same that was used to create the biomass forming a closed carbon cycle as mentioned earlier. That is one of the main advantages of utilizing biomass as an energy source versus fossil fuels which generates new greenhouse gases according to NREL (NREL 2014). The use of biomass as an energy form can be traced back to prehistoric times when wood was burned for energy. Furthermore, biomass has the potential to largely replace the heavily depended-upon fossil fuels and can be utilized in three useful ways. Biomass can be converted to liquid fuels termed biofuels which is the main focus of this dissertation effort. However it can also be directly burned for electricity (biopower) or can be reprocessed into chemicals (bioproducts) (NREL 2014).

CH_4 and CO_2, the two most prominent greenhouse gases, are the primary components of biogas as previously mentioned and have been increasingly emitted into the earth's atmosphere. According to the key world energy statistics, CO_2 emissions have been steadily increasing for the past 45 years, with more than 31.7 GT of CO_2 emitted in 2012 (EIA 2016c). At the current rate, it is expected that emissions can reach 45 GT by 2040 which may devastatingly and irreversibly increase the earth's temperature by 2°C (EIA 2016c). Therefore, it is crucial to find ways to decrease emissions of CO_2. Furthermore, methane, which is the second most abundant greenhouse gas is more powerful than CO_2 in that it is able to trap energy much more efficiently into the earth's atmosphere (EPA 2016c). In fact, over a 100 year period, pound for pound, methane has an effect 25 times greater on the earth's atmosphere than CO_2 (EPA 2016c). Therefore, methane is a gas that should be mitigated and considered for its harmful effects just like CO_2.

However, depending on the source of the biomass, the produced biogas which is roughly equal parts of the two major greenhouse gases methane and carbon dioxide, can also have some contaminants (EPA 2016b). In which case, a gas cleanup process is necessary prior to processing.

1.2 Municipal Solid Waste Biomass

In the case of biodegradable municipal solid waste (MSW) dumped in landfills, the generated biogas, called landfill gas (LFG), has roughly the same composition of methane and carbon dioxide as other types of biogases but also contains some impurities. Biogas derived from MSW has the same potential as an energy source. The EPA has recently set limits on emissions of CH_4 from landfills (EPA 2016b) as part of the landfill methane outreach program (EPA LMOP). As a result of the program, CO_2 and CH_4 emissions from landfills have been reduced by 39.5MMTCO_2e in 2014 (EPA 2016a). Although the LMOP initiative has curbed emissions of both CO_2 and CH_4, there is still a very long way to go before emissions are overall reduced to an acceptable limit that does not contribute to global warming. According to the EPA (EPA 2016c), 20% of CH_4 anthropogenic emissions come from landfills as previously discussed. It is estimated that the US generates more than 250 million tons of municipal solid waste (MSW) per year which mostly go to landfills (EPA 2016b). That is roughly equivalent to 4.3 lb/day of waste per person which is expected to increase with the growing population. Biomass, the biodegradable component of MSW (and primary source for biogas) accounts for about 215 billion cu.ft/year.

A typical small to midsize landfill containing 1 million tons of MSW will produce 12,000m^3/day of LFG and will continue at this level of production for 20-30 years (EPA 2016b). Currently less than 15% of MSW is utilized for energy. However LFG is instead used in three main ways, the gas gets flared, or burned for electricity or the CH_4 gets condensed (CNG). Most of these are inefficient ways of utilizing the full potential of LFG. For instance, burning the gas for electricity is only about 40% efficient. Furthermore, the incineration process produces more pollutants and greenhouse gases. Condensing the CH_4 may be useful for industrial uses, however it still leaves the issue of the carbon dioxide unresolved. Reforming LFG to H_2 and CO (syngas) is one attractive route to reduce greenhouse gas emissions and generate a usable feedstock. Syngas can be used as a feedstock for ammonia as well as methanol synthesis and can be upgraded to long chain hydrocarbons such as diesel and jet fuel using Fischer Tropsch synthesis (FTS) (reaction 1.5 below). Furthermore, upgrading landfill gas has many environmental benefits including reduction of greenhouse gas emissions, improving air quality and reducing fossil fuel dependence.

1.3 Types of Methane Reforming

There are several different routes for reforming of CH_4 which are generally used in industry to produce H_2 and CO (syngas). Reforming of CH_4 can be done using CO_2 as the oxidant, termed dry reforming, which is shown as reaction (1) (DRM). Methane dry reforming is attractive due to the lower cost making it more viable for use in FTS (Bradford and Vannice 1999, Damyanova *et al* 2009b). However, for the endothermic dry reforming of methane reaction, high temperatures (T>600°C) are a necessity for reaching desirable H_2:CO (syngas) ratios for FTS.

$$Dry\ Reforming: CH_4 + CO_2 \rightarrow 2CO + 2H_2 \qquad \Delta H° = 247.3\ {}^{kJ}/_{mol}\ CH_4 \qquad (1)$$

$$Steam\ Reforming: CH_4 + H_2O \rightarrow CO + 3H_2 \qquad \Delta H° = 206.3\ {}^{kJ}/_{mol}\ CH_4 \qquad (2)$$

$$Partial\ Oxidation: CH_4 + {}^{1}/_{2}\ O_2 \rightarrow CO + 2H_2 \qquad \Delta H° = -35.6\ {}^{kJ}/_{mol}\ CH_4 \qquad (3)$$

$$Water\ Gas\ Shift: CO + H_2O \rightarrow CO_2 + H_2 \qquad \Delta H° = -41\ {}^{kJ}/_{mol}\ CH_4 \qquad (4)$$

$$Fischer\ Tropsch\ Synthesis\ (FTS): \ nCO + \left(n + {}^{1}/_{2}\ m\right)H_2 \rightarrow C_nH_m + nH_2O$$

$$\Delta H° = variable \qquad (5)$$

Hydrocarbon fuel synthesis and oxygenate fuels can be produced using the syngas when combined with steam reforming (reaction 2) or the WGS reaction (reaction 4).

Dry reforming of CH_4 readily occurs at high temperatures as previously stated, (Rostrup-Nielsen *et al* 2002) which adds to the overall cost of the process on an industrial scale, as CH_4 is commonly parasitically combusted to generate the heat. The DRM reaction is thermodynamically predicted to not occur at temperatures below 350 °C with coking being the only possible pathway at such low temperatures (Bradford and Vannice 1999, Pakhare and Spivey 2014). Using heterogeneous catalysis to drive the DRM reaction to lower temperatures has the potential to decrease the cost making it industrially more feasible. For FTS to produce longer chain hydrocarbons (C10+), a H_2:CO ratio of 2:1 is necessary (Dry 2004, Dry 2002). Lower H_2:CO ratios can be used for alkenes as well as acetic acid and alcohol production (Mortensen and Dybkjær 2015). The target of the experimental portion of this study is to look at the effect of contaminants (mainly siloxanes) in the biogas on the activity and conversion temperature of both a low temperature (0.16 wt% Pt-1.3 wt% Ni-1.0 wt% Mg/$Ce_{0.6}Zr_{0.4}O_2$) as well as a high temperature (1.3 wt% Ni-1.0 wt% Mg/$Ce_{0.6}Zr_{0.4}O_2$) reforming catalyst.

Alternatively, methane can also be reformed via steam only in a process called steam reforming (SRM) (reaction 2). Very high H_2:CO ratios (>3) are produced via this route compared to other types of reforming as a result of the water gas shift reaction simultaneously occurring (reaction 4). The H_2:CO ratio can be adjusted to the desired ratio through utilization of the different reforming reactions together such as coupling dry reforming with steam reforming (bi-reforming, reactions 1 and 2) and/or partial oxidation of CH_4 (tri-reforming, reactions 1-3) (Hokenek *et al* 2012, Song and Pan 2004, Walker *et al* 2012, Zhang *et al* 2014).

1.4 Siloxanes

Siloxanes are the name of a class of C, Si, O, and H containing compounds (Dewil *et al* 2006, Surita and Tansel 2015a) incorporated into a variety of personal care products over the last couple of decades and have high enough vapor pressures to be in measureable and significant concentrations in LFG (see Table 1 for nomenclature and general properties) and are still emerging in use (Ajhar *et al* 2010, Dewil *et al* 2006). This trend is evident in the fact that the first siloxane removal patent was issued in 1999 (Ajhar *et al* 2010) and in regards to the exponential increase in articles and citations on siloxanes and landfill gas (see Figure 1). According to a recent review (Rucker and Kummerer 2015), the worldwide annual capacity of siloxanes is estimated to be several million tons (~5 as gathered from several sources, with ~ 20% produced each in China and EU) with a previous growth rate of 2% from 1998 to 2002 and a predicted growth rate 6.5% from 2012 to 2017. Also, siloxanes are the most common classroom VOC (Tang *et al* 2015).

Table 1: Nomenclature and Properties for Typical Volatile Siloxanes (adapted from (Surita and Tansel 2015a))

Compound	Formula	Label	MW (g/mol)	Vapor Pressure (kPa) [a]	Water solubility (mg/L) [b]
Trimethylsilanol	$C_3H_{10}OSi$	TMS	90.2	2.13	35,000
Hexamethyldisiloxane	$C_6H_{18}OSi_2$	L2	162.4	4.12	0.93
Octamethyltrisiloxane	$C_8H_{24}O_2Si_3$	L3	236.5	0.52	0.05
Decamethyltetrasiloxane	$C_{10}H_{30}O_3Si_4$	L4	310.7	0.073	0.007
Dodecamethylpentasiloxane	$C_{12}H_{36}O_4Si_5$	L5	384.8	0.009	3.1E-4
Hexamethylcyclotrisiloxane	$C_6H_{18}O_3Si_3$	D3	222.5	1.14	1.56
Octamethylcyclotetrasiloxane	$C_8H_{24}O_4Si_4$	D4	296.6	0.13	0.056
Decamethylcyclopentasiloxane	$C_{10}H_{30}O_5Si_5$	D5	370.8	0.05	0.017
Dodecamethylcyclohexasiloxane	$C_{12}H_{36}O_6Si_6$	D6	444.9	0.003	0.005

[a] Vapor pressure at T = 25°C

[b] Water solubility at T = 25°C

Anaerobic conditions are reached within one to three years, with peak LFG production being reached within five to seven years. LFG is produced for 20 to 30 years following MSW being landfilled (https://www3.epa.gov/lmop/documents/pdfs/pdh_chapter1.pdf). With this substantial lag time between landfilling and contaminant evolution, changes in LFG handling and addition of conditioning steps may be necessary in response to future changes in LFG composition.

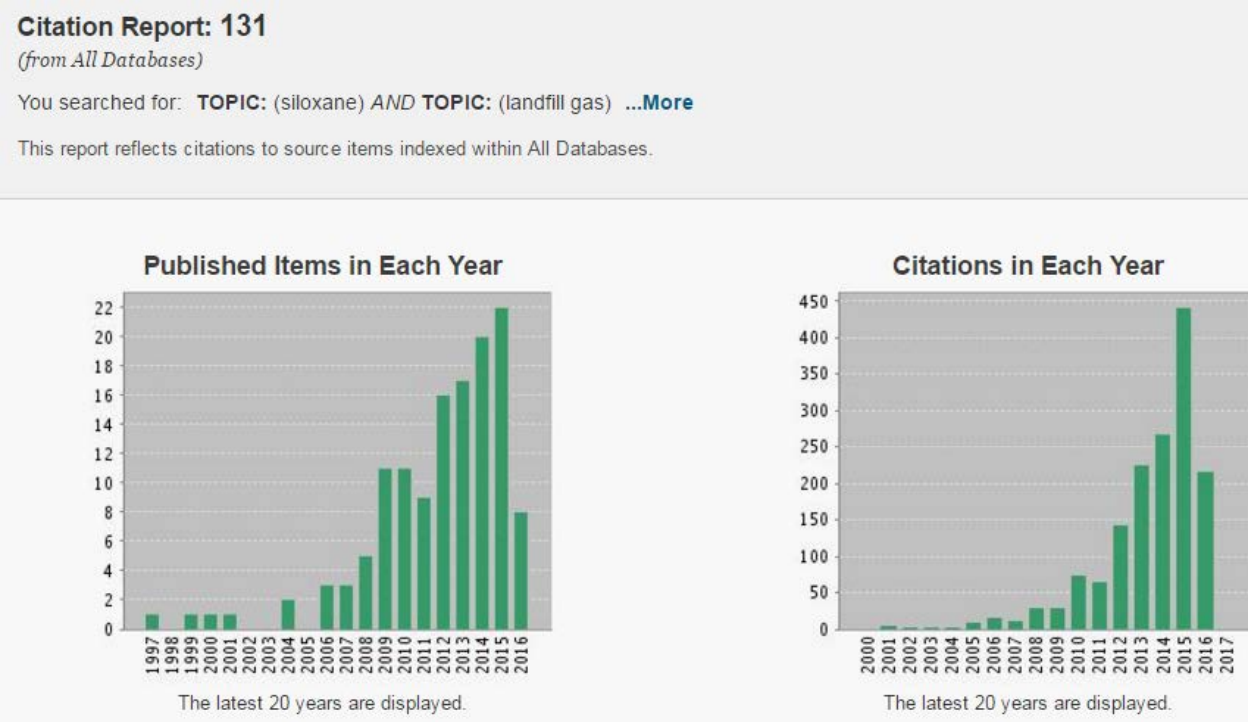

Figure 1: Search result via Web of Science for "landfill gas" and "siloxane", which shows limited number of research publications and citations and an exponential increase in these efforts. This increase is coupled to increased use of siloxanes in consumer products. Web of Science search and citation reported conducted on 8/23/16.

1.5 Typical LFG flowrates and contaminant compositions

In the U.S., the EPA Landfill Methane Outreach Program (LMOP) (EPA 2016d) and the EPA Greenhouse Gas (GHG) Reporting program are the primary databases for compilation of LFG collections. As noted by EREF and Dr. Bryan Staley at a 2016 SWANA meeting (Staley 2016), each program has its strengths and weaknesses. The LMOP is voluntary reporting for existing LFGTE projects and, thus, may neglect landfills that flare only. Since LFGTE projects would more likely be anticipated on large LFG flowrates, the statistics may be shifted toward the high end. Similarly, the GHG Reporting program only requires landfills to report LFG data if it produces more than 1000 metric tons of CH_4 annually. Using the LMOP here for illustration, the information contained in Table 2 is extracted.

Of the 976 entries reporting for distinct landfills, 880 (90.2%) disclosed LFG collection. Due to the wide range in reported values, it also seems worthwhile to mention that the median average would fall in the range of 1 – 3 mmscfd, with 2 mmscfd taken as a representative median value. The total LFG collected is 3070 mmscfd. Making the simplification of 50% methane (55.5

MJ/kg) in biogas, this total energy content is 6.3E8 GJ/yr or 107 Mboe/yr (the approximate amount of oil used worldwide per day). Assuming 20% efficiency in converting this chemical energy to electrical energy, it is enough to power 3.2 million homes. Regardless of the comparison, a substantial amount of energy is available to displace existing sources.

Table 2: Analysis of U.S. LFG collection via EPA Landfill Methane Outreach Program (LMOP)[a]

	LFG Collected			LFG flared		
	(mmscfd)[b]	(scfm)[c]	(Nm^3/min)	(mmscfd)	(scfm)	(Nm^3/min)
Maximum	45.1	31300	886	8.1	5630	159
Average (Mean)	3.49	2420	69	0.68	470	13
Representative Median	2.0	1390	39	0.4	280	7.9
Minimum	0.050	35	1.0	0	0	0

[a] database downloaded from LMOP on 7/14/2016.

[b] millimeter standard cubic feet per day

[c] standard cubic feet per minute

Another major source of biogas is from cleanup at wastewater treatment plants (WWTPs). Although the biogas flow rates vary widely, the typical values are much smaller at WWTPs than landfills. For example, in Europe, biogas production at WWTPs ranges from 1560 to 29500 m^3/day (38 to 723 SCFM) (Raich-Montiu *et al* 2014). When compared to the values of Table 2, it is becomes evident that individual projects for WWTPs would have a much smaller impact than landfills.

Similarly, there is also a wide variety of LFG contaminant compositions. In addition to the roughly 50% methane, 45% CO_2, O_2 and N_2 from air (mainly from the blower), and saturated amounts of water, the contaminant amounts largely depend on the composition of the MSW being landfilled. A number of publications (examples (Arnold 2009, Hill 2014, Papadias *et al* 2012)) have superbly reported on the composition of LFG. A literature survey on the

composition of landfill gas was also conducted for this review and the detailed tables are contained in the supporting information.

The concentrations of siloxanes can be much higher in biogas from WWTPs than in LFG. As reported by Hill et al (Hill 2014), the highest values for LFG and WWTP biogas are 4 ppmv (~ 67 mg/Nm^3) and 25 ppm_v, (~ 417 mg/Nm^3), respectively. In biogas derived at WWTPs in Europe, total siloxane concentrations as high as 127.4 mg/Nm^3 have been reported (Raich-Montiu *et al* 2014). These high values for WWTP biogas are factors of ~ 10 to 20 than those on the high end of LFG (see Table 3; 15 mg/Nm^3). A word of caution on siloxane concentrations is that both ppm_v and mass concentration are used throughout the literature and the specific compounds are not noted to make precise conversions.

Table 3: Typical contaminant concentrations in LFG. See supporting information for details.

Class of compounds	**Molar mass (g/mol)**	**Typical Concentration Range (mg/m^3)**
Siloxanes (L2-D5)	162-371	0.005-15
Sulfur compounds: (H_2S-CH_4S)	34.1-48	0.56-280
Chlorides (CCl_4-C_2HCl_3)	112-166	0.14-4.52
VOCs (Benzenes, isopropyl benzene, halogenated compounds)	78-120	0.85-5.6
Alkanes/ alkenes (C_7H_8-$C_{16}H_{34}$)	92-226.4	0.1-85.3
Mercury compounds (CH_3Hg-$(CH_3)_2Hg$)	216-231	1-91E-3

Regardless, the two important classes of contaminants requiring further downstream processing are sulfur species and siloxanes, which will become more evident in the next two sections (contaminant tolerances for LFGTE processes and contaminant removal technologies). In brief, these two classes of contaminants lead to substantial processing challenges and irreversible

damage even at low concentrations and require removal technologies. H_2S is the primary sulfur containing species. For these reasons, H_2S and siloxanes are highlighted in Table 4, which presents typical and highest reported (de Arespacochaga *et al* 2014, Dewil *et al* 2006, Papadias *et al* 2012, Raich-Montiu *et al* 2014, Schweigkofler and Niessner 2001, Tansel and Surita 2013) concentration values in both LFG and WWTP biogas.

Table 4: Comparison of highest reported and typical values for key contaminants

Biogas	Contaminant	Concentration		References
		Highest	Typical	
LFG	H_2S	5400 ppmv	63 ppmv	Papadias et al, 2012
	Siloxanes	54 mg/Nm^3	16.8 mg/Nm^3	Tansel and Surita, 2013/ Schweigkofler and Niessner, 2001 / Dewill et al 2006
WWTP	H_2S	3 %	400 ppmv	Arespacochaga et al, 2015/ Papadias et al, 2012
	Siloxanes	400 mg/Nm^3	46 mg/Nm^3	Dewill et al 2006 / Raich-Montiu, 2014

As alluded to earlier, several technologies are available to harness the energy content of LFG. These LFGTE processes a variety of methodologies (turbines, engines, fuel cells) to produce electricity, chemical processing to produce vehicle fuels (LNG, CNG, synthetic hydrocarbon liquids), or injection of purified biomethane into the natural gas grid. Each of these techniques has its own tolerance to contaminants. Moreover, components of LFG could be viewed as reactants in certain cases, inerts in others, and even contaminants in selected cases. This point can be best made using CO_2 as an example. CO_2 may be an oxidant for methane reforming in the

case of solid oxide fuel cells (SOFCs) and in synthetic fuel production, an inert for turbines and engines, and an impurity for injection into the natural gas grid. Similar assessment could be made for certain NMOCs. Regardless, a comparison of the permitted contaminants' concentrations are known in many scenarios and compared in Table 5. However, due to the wide variety and sheer number of trace components, tolerances to every potential contaminant are not established.

2. ACCEPTABLE CONTAMINANT TOLERANCES FOR LFGTE PROCESSES

The results of Table 5 provide a summary of the most common and established LFGTE processes. A broader view, which includes many low tech approaches such as domestic stoves and boilers, can be found elsewhere (Sun *et al* 2015). After noticing that a number of contaminant tolerances are not known for the respective LFGTE technologies, another noticeable item is the wide range of gas conditioning required. For example, tolerances for engines and turbines are much more forgiving than for fuel cells and purified CH_4applications (vehicle fuel and pipeline). Note that 1 mg H_2S/Nm^3 CH_4 is approximately 0.5 ppm_v if CH_4 is ~ 60% of the total gas. Due to the separation of the LFG and the working fluid, Stirling Engines are the most forgiving. A similar trend for H_2S is also observed for siloxanes. Since fuel cells use catalyst technologies, the low tolerance of contaminants relative to engines and turbines is a logical deduction.

By comparing contaminant levels in the feed (Table 4) with the removal required (Table 5), siloxanes become the key contaminant requiring removal even though the amounts of H_2S are higher compared to siloxanes. This result is evident as a number of recent studies (Álvarez-Flórez and Egusquiza 2015, Haga *et al* 2008, SEPA 2004, Sevimoglu and Tansel 2013b, Surita and Tansel 2015b, Urban *et al* 2009), which have discussed engine damage caused by siloxanes, whereas damage by sulfides is less common. Although H_2S removal is required for fuels cells and vehicle fuel applications, it is not necessary for engines unless the concentration gets above at least ~350 ppm_v (Waukesha ICE, and assuming 60% CH_4 by volume), with another factor of 3 higher tolerance for the other ICEs. Alternatively, siloxane removal would likely be necessary from LFG for certain technologies, depending on the feed values and the LFGTE tolerances. Again, tolerances for engines are higher than for fuel cells and injection into the grid, which again highlights siloxane removal as a key gas conditioning effort for selected technologies. The

timeliness of siloxanes as a pollutant is also evident as the tolerance of fuel cells was not determined until the last decade (Gadde 2006).

Table 5: Tolerance of LFGTE processes to key contaminants

LFGTE process [a]	**Manufacturer / Type**	**Contaminant Tolerance**				**Reference**
		H_2S (mg/Nm^3 CH_4)	Siloxanes (mg/Nm^3 CH_4)	Halides (mg/Nm^3 CH_4)	Ammonia (mg/Nm^3 CH_4)	
Internal Combustion Engine	Caterpillar		28 [b]			Wheless and Pierce, 2004; de Arespacochaga et al, 2015
		2140	21	713	105	SEPA, 2004
	Jenbacher		10 [b] / 12 [b]			Wheless and Pierce, 2004; de Arespacochaga et al, 2015
		1150	20	100	55	SEPA, 2004
	Waukesha		25 [b] / 30 [b]			Wheless and Pierce, 2004; de Arespacochaga et al, 2015
		715	50	300		SEPA, 2004
	Deutz		5 [b]			Wheless and Pierce, 2004
		2200	10	100		SEPA, 2004
	Tech3solution		5 [b]			Wheless and Pierce, 2004; de

						Arespacochaga et al, 2015
Turbine	Solar Turbines		0.1 [b]			Wheless and Pierce, 2004
	IR Microturbines		0.06 [b]			Wheless and Pierce, 2004
	Capstone Microturbines		0.03 [b]			Wheless and Pierce, 2004; de Arespacochaga et al, 2015
Stirling Engine	n/a		No limit			de Arespacochaga et al, 2015
Fuel Cells	MCFC	1-5 [c]		Few ppm		Sun et al, 2015
	PAFC		0.05-0.1 [b]			de Arespacochaga et al, 2015
	SOFC	1 [c]		Few ppm		Sun et al, 2015
Natural Gas Grid [c]	(varies by country)		0.5-10 [b]			de Arespacochaga et al, 2015
Vehicle Fuel [b]	n/a	5 [b]				Sun et al, 2015

[a] All LFGTE technologies require some degree of water removal

[b] mg/Nm^3 (i.e., per total LFG volume, not per CH_4 partial volume as stated)

[c] ppm (not per CH_4 partial volume as stated)

[d] requires substantial CO_2 and air removal

Several articles have examined the tolerance of SOFC anodes to hydrogen sulfide and siloxanes in the last decade. In 2008, Shitori et al determined that 1 ppm H_2S caused 9% voltage drop at 1000°C and the performance loss was reversible (Shiratori *et al* 2008). Although 1 ppm is used as a general tolerance value, the same authors determined the poisoning effect was much worse when operating at 800°C (Shiratori *et al* 2010). Since a desire exists to lower the operating temperature due to material compatibility issues, the 1 ppm H_2S tolerance is more of a guideline than a rule. In addition, recent studies on siloxane contamination have been reported. Ni anodes have initial performance losses at 10 ppb_v (Papurello *et al* 2014), which is ~ 0.165 mg/Nm^3. Device failure occurred at 10 ppm_v (of D5; 165 mg/Nm^3) within 20-30 hr (Haga *et al* 2008). As noted, siloxanes decompose to silica and, thus, it is irreversible damage even at low amounts such as 5 ppm_v D4 (66 mg/Nm^3) (Madi *et al* 2015). While siloxane decomposition is generally regarded as irreversible, regeneration of Pt-based oxidation catalysts for waste flue gas combustion from waste incineration plants has been reported (Rasmussen *et al* 2006). Since siloxanes are an emerging contaminant and their removal is becoming more necessary, additional studies on the operation conditions and performance losses are needed for many of the LFGTE processes.

2.1 LFG current cleanup technologies

LFG derived from MSW contains a variety of impurities that must be cleaned prior to the reforming process. Otherwise these contaminants rapidly build up in equipment (engines, turbines…etc.) causing it to fail as well as deactivate reforming catalysts and are harmful to the environment. Contaminants present in LFG include siloxanes, sulfides, halides and mercury compounds. This study focused on siloxanes as mentioned earlier. Siloxanes decompose to silica, which then deposits onto the equipment and/ or catalyst causing irreversible damage. To protect the equipment from the extensive damage these siloxanes can cause, engine manufacturers have decreased the allowable siloxane concentration limits to maintain warranty (Kuhn *et al* 2017). This fueled the need to have efficient cleaning processes. Currently, industrial contaminant removal can be categorized into three main areas, adsorption, absorption and chilling (Dewil *et al* 2006).

2.1.1 Adsorption

A number of the recent articles primarily review the basic functions and performance of typical unit operations for purifying biogas (Bioenergy, Dewil *et al* 2006, Estefanía López *et al* 2012, Ryckebosch *et al* 2011, Yang *et al* 2014). Ajhar et al recently summarized a number of commercial and patented siloxane removal technologies (Ajhar *et al* 2010). In their analysis (Ajhar *et al* 2010), the fate of the siloxanes can vary for fixed bed adsorption between release to the atmosphere, being flared, or disposal with spent adsorbent media depending on the specific commercial process. A careful balance between the economic, environmental, and regulatory considerations is certainly important as the fate of the contaminants is determined.

Sun et al is the only review that includes methane losses (Sun *et al* 2015). While it considers methane losses during CO_2 removal, it is amazing to see CH_4 losses as high as 20% (for membrane separations) reported (Sun *et al* 2015). Typical values for CH_4 losses by conventional techniques are ~ 5%, with chilling/refrigeration and chemical methods having lower values than physical absorption (Sun *et al* 2015).

Recent research has also brought new materials and processes for contaminant removal. To enhance the phase change of siloxanes to silica and thus decrease the mobility (as spent sorbents may be landfilled), high temperature adsorption materials have been used as guard beds. The term high temperature polisher has also been used to describe this operation (Papadias *et al* 2012). These materials are essentially guard beds (almost “disposable catalysts” to facilitate decomposition) to provide a surface for siloxane removal. Finocchio et al compared alumina, silica, magnesium oxide, and calcium oxide at T = 673 K and determined 0.31 g siloxane/g alumina (Finocchio *et al* 2008). Basic oxides (CaO and MgO) faced too much competition from CO_2 when present (Finocchio *et al* 2008). Similarly, Urban et al identified alumina from a material screening study (Urban *et al* 2009).

Switching back to conventional adsorbents, different approaches are taken in the literature. First, novel materials designed for high adsorption capacities are being developed. Second, conventional adsorbents are being tested for this application. Recent contributions on both of these aspects, as well as adsorbent regeneration, are described here.

The Suib group at UCONN has recently researched the application of superhydrophobic mesoporous polymeric adsorbents and reported capacities as high as 2370 mg D4/g media (Jafari *et al* 2015). The developed adsorbent had a capacity of 1.6 to 2.5 times that of a commercial activated carbon and humidity and CO_2 did not have a major impact on the capacity, unlike that of the commercial activated carbon (Jafari *et al* 2015). Moreover, the adsorbent was regenerated via heat treatments in air at 100°C overnight and used up 5 times with only minimal (less than 10% capacity loss) impact (Jafari *et al* 2015). This group also compared capacity of modified mesoporous silica to commercial silica and found D4 adsorption capacity (642 mg D4 / g media for commercial silica versus 686 mg D4 / g media for optimized silica) (Jafari *et al* 2016). These approaches of using hydrophobic materials follows the work by Mito-oka et al, who initiated research for siloxane separation with this approach but with the comparison not quantified (Mito-oka *et al* 2013). Most recently, the Suib group reported the capacity of mesoporous aluminosilicates to be as high as 105 mg D4/g media (Jiang *et al* 2016). These recent publications indicate the wide range of capacities possible even in simulated biogas studies and the potential detrimental impact of other biogas components such as CO_2 and moisture. Although promising, the long-term use of these materials including regeneration in the presence of multiple contaminants need validated.

Although not necessarily having the highest capacity, silica adsorbents are often considered better than other techniques (Schweigkofler and Niessner 2001). However, others have concluded that activated carbon is the most suitable adsorbent (Montanari *et al* 2010). Carbon-based adsorbents, in particularly activated carbon, are the most studied and are frequently demonstrate the highest uptake capacities. Although adsorbent capacity was not studied, activated carbon was been shown effective in limiting siloxane deposition on engine components (Sevimoglu and Tansel 2013a) and demonstrated to remove up to 52% and an average of 17% of siloxanes from digester gas at a Miami-Dade wastewater treatment facility (Tansel and Surita 2013).

Finochio et al determined activated carbon (570 mg/g media) to have higher capacity than inorganic materials (silica gel, 230 mg/g media; Faujasite zeolite, 276 mg/g media) and most modified activated carbon adsorbents (Finocchio *et al* 2009). In addition, the activated carbon had a significant drop (factor of 2 or 8 depending on bed location) in capacity upon reuse. In a

follow up study, a higher regeneration ability for Faujasite zeolite (16 to 23%, depending on temperature) than activated carbon (4 to 8%) was reported, with no regeneration possible for silica gel (Montanari *et al* 2010). Ortega and Subrenat measured from 300 to 400 mg siloxanes/g media, depending on the specific conditions for different types of activated carbon, and lower values for zeolite and silica gel adsorbents (Ricaure-Ortega and Subrenat 2009). They also determined negative effects of increasing humidity and increasing temperature. After the first cycle, further decreases in the breakthrough time were not reported. Matsui and Imamura determined the adsorption capacity of many activated carbon samples (range from 56 to 192 mg D4/g media) and molecular sieves (range from 4 to 77 mg D4/g media) and silica gel (104 mg D4/g media) and demonstrated removal of siloxanes from real digestion gas for two types of activated carbon adsorbent for up to 1000 hr (Matsui and Imamura 2010). A similar study was also published by Oshita et al, who reported respective D4 and D5 uptakes ranging from 51 mg D4/g media and 52 mg D5/g media (zeolite) to 404 mg D4/g media and 531 mg D5/g media (activated carbon) (Oshita *et al* 2010). Gilson et al also tested several types of activated carbon and determined that the best performing one decreased capacity for L2 adsorption from ~110 to ~ 75 mg L2/g media upon 2 thermal regeneration cycles (Gislon *et al* 2013). Cabrera-Condony et al reported a range from 249 to 1732 mg D4/g media at 1000 ppm_v D4 in dry N_2 with the best performing material maintaining substantial capacity (897 mg D4/g media) in simulated biogas containing 1.45 ppm_v D4 (Cabrera-Codony *et al* 2014).

Studies to this point agreed that activated carbon had the highest capacities. However, in the most recent series of screening studies, Sigot et al demonstrated silica gel (216 to 260 mg D4/g media) to have the highest adsorption capacity while activated carbon (52 to 53 mg D4/g media) had minimal uptake when tested at 30 ppm_v D4 (Sigot *et al* 2014, Sigot *et al* 2016). The lowest report of adsorption capacity of siloxanes on carbon was 4 mg siloxanes / g media (Wheless and Pierce 2004). The activated carbon that both Sigot et al (Sigot *et al* 2014, Sigot *et al* 2016) and Wheless and Pierce (Wheless and Pierce 2004) describe is coconut-based, so perhaps there is some unique feature of this material that limits siloxane adsorption. These results indicate that, although the nature of adsorbent is important (adsorption capacity varies by factor of ~ 3 (Matsui and Imamura 2010, Oshita *et al* 2010) and ~7 (Cabrera-Codony *et al* 2014) in these screening studies comparing at the same conditions in respective studies), the conditions also seem very important.

Several challenges exist in design adsorption operations of siloxanes. First, adsorbent capacities vary widely among studies even of similar materials. At least in part, this could result from differences in materials and conditions. Feed composition (including siloxanes concentrations) vary widely, and also temperature, pressure, relative humidity are scarcely reported. Hepburn et al contributed the differences for breakthrough times and capacities through sensitivity of various analytical equipment (Hepburn *et al* 2015). Second, issues related to regeneration are not solved despite recent patents insinuating progress (de Arespacochaga *et al* 2015). The challenge may be overbearing since siloxane conversion to other species (silica and silicon) has been identified (Boulinguiez and Le Cloirec 2010, Cabrera-Codony *et al* 2014, Finocchio *et al* 2009, Sigot *et al* 2015). Third, many studies report breakthrough times and/or adsorbent capacity rather than isotherm data, which is the commonly needed for designing an adsorption bed. Limited studies report isotherms, such as Langmuir-Freundlich (Boulinguiez and Le Cloirec 2010), Freundlich (Ricaure-Ortega and Subrenat 2009), and Dubinine- Radushkevich (Papadias *et al* 2012) isotherms. Moreover, there may be confusion over whether breakthrough or equilibrium adsorption capacity is reported. Ortega and Subrenat reported both and the equilibrium adsorption capacity is approximately 5x larger than that for the breakthrough adsorption capacity (Ricaure-Ortega and Subrenat 2009). Fourth, the studies that do report isotherm data are based on simulated (i.e., clean) feeds rather than multi-component adsorption. As activated carbon and silica adsorb many biogas contaminants (Boulinguiez and Le Cloirec 2010), competitive adsorption will limit individual capacities during multi-component adsorption (Hepburn *et al* 2015, Sigot *et al* 2015). Finally, preferential adsorption results in weakly bound molecules being replaced by more strongly bound species. Consequently, high amounts of specific species (the weakly bound ones; L2 especially) are concentrated in the effluent (Wheless and Pierce 2004).

2.1.2 Absorption

The second major type of contaminant removal is absorption which is also a continuous process that can be either chemical or physical. Chemical absorption utilizes strong acids and bases such as sulfuric acid or sodium hydroxide. Physical absorption is done using absorbents as well as organic solvent (Ajhar *et al* 2010). Packed or spray columns are the most widely used for siloxane absorption. However, gas flow rate plays a key role in amount of siloxane removed.

Where at higher flowrates, the siloxanes can flow out of the solvent and back into the gas defeating the process of removal (Dewil *et al* 2006).

2.1.3 Gas Chilling

The final major technology used for contaminant removal is gas chilling. Removal is done at a temperature less than -25°C where larger siloxanes are condensed (Ajhar *et al* 2010). However, all of these removal technologies add high operating costs to the process such as frequently replacing scrubbing beds. In addition, as discussed earlier in this section, engine manufacturers are implementing more stringent warranty guidelines for allowable VMS levels. This in turn forces the need for higher contaminant removal levels and better technologies which still need to be developed to make the process economical.

2.2 Cost Comparison

Although many removal techniques and sorbent regeneration strategies may prove effective, economical consideration ultimately are an immense factor. As examples, similarity and familiarity with the economy-of-scale challenges of natural gas conversion are one indicator. As a result, subsidies and incentives are often required to promote market disruption. There are many examples, with recent case studies from the Netherlands (Gebrezgabher *et al* 2010) and Ireland (Czyrnek-Delêtre *et al* 2016). Even so, a recent report (Hill 2014) has estimated the payback period for siloxane removal to be from 0.5 (0.5 to 9 ppm_v), 1.0 (9 to 25 ppm_v), 2.0 (25 to 60 ppm_v) to 3 (60+ ppm_v) years depending siloxanes concentration ranges stated. This report (Hill 2014) also substantiates the saving for lean burn engines through various terms such as spark plug and check valve lifetime extensions, power savings, less frequent engine re-builds and oil changes. Sun at al has estimated the energy requirements and process efficiencies for various removal technologies. (Sun *et al* 2015) Another earlier review have categorized costs per high, medium, or low for CAP-EX and OP-EX based on these ranges: CAP-EX (k€/Nm^3/h) - <0.5 (low), 0.5–1 (medium), 41 (high); OP-EX (c€/Nm^3) - <1.5(low), 1.5–3 (medium), 43 (high) (de Arespacochaga *et al* 2015). The present work is the first to compile literature costing analyses on a gas volume processed and contaminant removed bases.

A tabulation of literature findings of gas conditioning costs are in Table 6. From the results of Table 6, the costs on a gas volume process ranged from <$0.01 to $0.13/$Nm^3$. On total masses of contaminants removed, the costs ranged from $2.17/kg to $271/kg. This range may not be

substantial in terms of large engineering projects. The primary reason for the range is that dilute contaminants on a small scale cost more to remove on a mass of contaminants removed basis than concentrated contaminants on a large scale. That is, there is both an economy-of-scale and a phenomenological (kinetics and thermodynamics) influence. The detailed case studies by Arnold report the lowest costs (Arnold 2009). The costs are the values reported in the respect studies updated to USD and to 2016 (via inflation), unless noted in the text. While some costs are through a complete economic analysis, others are levelized costs, which are the OP-EX plus the CAP-EX divided by years of operation. It is a simplified economic term taking into account both expenses but without the prediction and uncertainty of the time value of money. An example for the estimate of the annualized cost based on one study is provided below. For comparison, several established H_2S removal techniques are included, noting there is not enough information provided in those references to permit a cost on both the gas volume and contaminant mass bases.

Although many factors are involved with the estimates in each study, costs for adsorption generally scale linearly rather than a lower value such as the general “6 tenths” estimate due the high OP-EX relative to CAP-EX. An example for H_2S adsorption on Fe materials is here (Papadias *et al* 2012). For this reason, the fairness of comparing the costs in Table 6 is more reasonable than for other processes.

As expected, the cost tends to increase as the number of processing units increase. This is evident in few studies including combinations of drying, Fe-based sorbent, activated carbon, and biotrickle filter (BTF) (de Arespacochaga *et al* 2014) and additional activated carbon bed at end of biological sulfur removal and drying (Gadde 2006). In part, factors could involve local regulations, as well as the specific LFGTE process. For example, in one of the earliest analyses, Gadde indicated 100 ppm H_2S remained and no effort for ammonia removal was necessary for combined heat and power, whereas the ammonia must be removed and the H_2S concentration had to be lowered to 10 ppm for fuel cell applications.

In a recent thesis from the University of South Florida (Kent 2016), a costing analyses of the overall process was performed for a LFG flow of 2500 SCFM to be used for diesel fuel production. For CAP-EX, the total costs was estimated to be $1.6E6 (~15% of the total plant

costs) and included funds for compressor, heat exchangers, and adsorption beds. An additional 17% installation costs were added to reach $1.9E6. Annually, OP-EX included 10% of the installed costs, 25% of the total labor and utilities, and adsorbent replacement to reach a total of $1.273E6 per year. Assuming 10 years of operation, the levelized cost (CAP-EX / 10 years + OP-EX =) of $1.463E6. The costs are then $0.04/$Nm^3$ and $33/kg. In terms of gas volume basis, this result is approximately the average of these two previous values.

Sticking with these three studies because they basically reflect the lowest (~$0.01/$Nm^3$) (Gadde 2006), highest ($0.13/$Nm^3$) (de Arespacochaga *et al* 2014), and an average cost on a LFG volume basis, the levelized costs can vary from $0.24E6 to $2.2E6 per year, assuming 10 years of operation and a flow rate of 2500 SCFM (rounding a mean LFG value from Table 4). There is an order of magnitude variation in these values, which represents a more refined analysis is required to firmly predict costing. Second, depending on the LFGTE process to some extent, the values represent a substantial fraction of the profits to cover the purification costs.

Table 6: Cost analyses of biogas purification

LFG flowrate (Nm^3/min) [a]	**Contaminant (Concentration)**	**Technology**	**Cost per volume ($/$Nm^3$) [b]**	**Cost per mass contaminant removed ($/kg) [b]**	**Reference**
70.8 [c]	H_2S (700 ppm) Siloxane (15 mg/m^3)	Iron sponge, AC bed	0.04	33.0 (~88% H_2S)	Kent, 2016
1.36	H_2S (2000 ppm) Siloxane (n/a)	biological sulfur removal and condensation	0.01	2.17 (100% H_2S)	Gadde, 2006
“	“	Previous + 2 carbon beds	0.02	6.39 (100% H_2S)	Gadde, 2006
3.17	H_2S (3000 ppm) Siloxane (14 mg/m^3)	Optimized BTF + drying, Iron sorbent, + AC	0.04	8.50 (~97% H_2S)	de Arespacochaga et al, 2014

“	“	BTF + drying, Iron sorbent, + AC	0.06	12.8 (~97% H_2S)	de Arespacochaga et al, 2014
“	“	Drying , Iron Sorbent, + AC bed	0.13	27.6 (~97% H_2S)	de Arespacochaga et al, 2014
1.8	H_2S (400 ppm) Others not quantified	Iron sponge, condenser, AC bed. & HT polisher	0.06	82 (~2% Si, ~0.4% Cl, 97% H_2S)	Papadias et al, 2012
2.2	H_2S (62 ppm) Others not quantified	“	0.04	271 (~1% Si, ~30% Cl, 69% H_2S)	Papadias et al, 2012
0.94	H_2S (1000 ppm)	Fe adsorbent	0.03	6.6 [d]	Abatzoglou and Boivin, 2009
“	H_2S (1000 ppm)	Na_2CO_3 /AC	0.04	22.5 [d]	Abatzoglou and Boivin, 2009
133	H_2S (600 ppm) Siloxanes (0.5-1 ppm) Halogen (~5 ppm)	Varies (catalytic scrubbing, bio and biochemical scrubbing, and carbon and resin adsorption)	<0.01		Arnold, 2009
“	“	Condensation and adsorption	0.025		Arnold, 2009
Comparisons					
	H_2S only	AC bed	0.02 – 0.03		Mescia et al, 2011
	H_2S only	SulFerox		0.24-0.30	Mota et al, 2011

	H_2S only	H_2SPLUS (225 kg/d max)		2.20 (OP-EX only)	Mota et al, 2011
	H_2S (1000 ppm)	Sulfatreat	0.03	17.7	Abatzoglou and Boivin, 2009
	H_2S only	LoCat		0.45-1.2 (OP-EX only)	Arnold, 2009
	H_2S only	Biological desulfurization		0.11 to 0.28	Sun et al, 2015
	H_2S only	Iron chloride		0.96	Sun et al, 2015
	H_2S only	Impregnated activated carbon		4.34	Sun et al, 2015

[a] 1 Nm^3 = 35.3 SCF

[b] All monetary values adjusted to 2016 USD, which could involve both a Euro to USF conversion and a time value of money correction. Rounded to 2 decimal places.

[c] As reference points of 700 ppm H_2S at 70.8 Nm^3/min (2500 SCFM), 108 kg S/day removed and daily flow is 1E5 Nm^3/day. From the sulferox fact sheet this makes it the most reasonable, which is in agreement with this review (Mota *et al* 2011).

At 600 SCFM or 17 Nm^3/day, the daily flow is 2.5E4 Nm^3/day. At 700 ppm H_2S, the amount of Sulfur removed per day is 26 kg. From the fact sheet, this is in the disposable adsorption area.

This report specifies 35 ppm as US LFG average. (Arnold 2009) Using this average, the amount of sulfur removed decreases to 1.3 kg/day (at 600 SCFM) and 5.4 kg/day (at 2500 SCFM).

[d] A value seems incorrect in the reference, as the amount of adsorbent is 5 x greater amount , but 40 % less capacity.

3. CATALYST SYSTEM

This study looked at poisoning effects in a high temperature catalyst comprised of nickel (1.34wt%) and magnesium (1.00wt%) on a ceria zirconia oxide support (0.6:0.4 mass ratio). In addition, a low temperature reforming catalyst comprised of the same components but also doped with platinum (0.16% by mass) was studied for effect of poisoning. The support and components of the catalyst system used for the experimental portion of this work has been described in great detail in a previous study, including both Hinkley reports by this group as well as published literature (Elsayed *et al* 2016, Elsayed *et al* 2015, Walker *et al* 2012), and will be discussed briefly in the next sections.

3.1 Ceria-Zirconia Oxide Support

Ceria is a widely used support as a result of its high oxygen storage capacity (OSC) which improves the reducibility thereby helping progress the reaction (Laosiripojana and Assabumrungrat 2005). In addition, coking is reduced as a result of the present oxygen vacancies in the support (Ruiz *et al* 2008). Zirconia improves the redox properties through enhancing the mobility of oxygen resulting from its smaller ionic size which creates a lattice strain (Ruiz *et al* 2008, Walker *et al* 2012).

3.2 Nickel Catalysts

Nickel is a heavily used catalyst on an industrial scale because it offers several attractive features including high activity, abundance and feasible cost. For methane reforming (dry and steam), nickel catalysts on ceria-zirconia have been shown to produce H_2:CO ratios between 650°C and 900°C (Laosiripojana and Assabumrungrat 2005, Song and Pan 2004).

3.3 Magnesium

Addition of magnesium oxide (MgO) to nickel oxides have been shown to decrease coke formation and Ni agglomeration (Bradford and Vannice 1996). Reducing coke formation and agglomeration helps maintain catalyst activity as coking is known to deactivate nickel catalysts.

3.4 Noble Metals

Noble metals including Pd, Ru, Rh or Pt which is used in this study, are commonly used as dopants to nickel catalysts. Platinum helps reduce the oxide phases through its affinity to facilitate dissociative hydrogen adsorption. Hydrogen has been identified to adsorb and

dissociate on the surface of the platinum whereby it spills over to the entire surface of the ceria (Dantas *et al* 2010). There is a direct correlation between reduction temperature and catalytic activity with higher activity associated with lower reduction temperatures.

4. EXPERIMENTAL PORTION

4.1 Synthesis and Materials

The commonly used co-precipitation method was utilized in the synthesis of the $(CeZr)O_2$ support and discussed in greater detail in a previous studies (Elsayed *et al* 2016, Elsayed *et al* 2015, Walker *et al* 2012).

Batches of 12 g were synthesized each time by weighing ~8.7g of the cerium precursor $Ce(NO_3)_3$ x $6H_2O$-(99.5% pure; Alfa Aesar) and ~3.3g of zirconium precursor $ZrO(NO_3)_2$ x H_2O-(99.9% pure; Alfa Aesar). After initially dissolving the precursors in deionized water, 75 mL of ammonium hydroxide (28% w/w NH_3; Sigma Aldrich) was slowly added while stirring to precipitate the precursors. A vacuum filtration step followed prior to dissolving the filtrate in 0.25M NH_4OH solution and vacuum filtering a second time. The filtrate was initially dried for 1hr at 60°C followed by 12 hr at 120°C before finally calcining at 800°C for 4 hr.

The metals were loaded using incipient wetness impregnation using the nickel precursor $Ni(NO_3)_2$ x $6H_2O$ (99.9985% pure; Alfa Aesar), the magnesium precursor $Mg(NO_3)_2$ x H_2O (99.999% pure; Alfa Aesar), and the platinum precursor H_2PtCl_6 x $6H_2O$ (≥37.5% metal basis, Sigma-Aldrich. The metal precursors were weighed and dissolved in deionized water and added dropwise onto the support until incipient wetness. The wet powder was then dried at 120°C for 2 hr and the process was repeated until all the metal solution was used where the final drying step was followed by a calcination at 600°C for 3 hr.

Catalyst poisoning was done in a manner similar to wet impregnation. The desired mass of catalyst is weighed in a ceramic boat. The necessary amount of Ludox® which is a colloidal silica suspension (40 wt% suspension in water, Sigma-Aldrich) is weighed in a vial and DI water is added to thin the Ludox® (about 1.5 mL for every gram of Ludox®). The Ludox solution is then added dropwise unto the catalyst until incipient wetness. The catalyst is then placed in a heated oven at 350° for 15 minutes. The process is repeated until all the Ludox® solution is used up. Upon final drying the catalyst is then calcined at 600°C for 4 hours. The resulting powder is

shown in Figure 2(b), which can be compared to the unpoisoned catalyst in Figure 2(a). A second batch of the NiMg only catalyst was done using the same method described but was calcined at 800°C to determine if a change in surface area and/or bulk properties would occur for the high temperature catalyst based on calcination temperature. Figure 3 shows a schematic of poisoning on the catalyst surface.

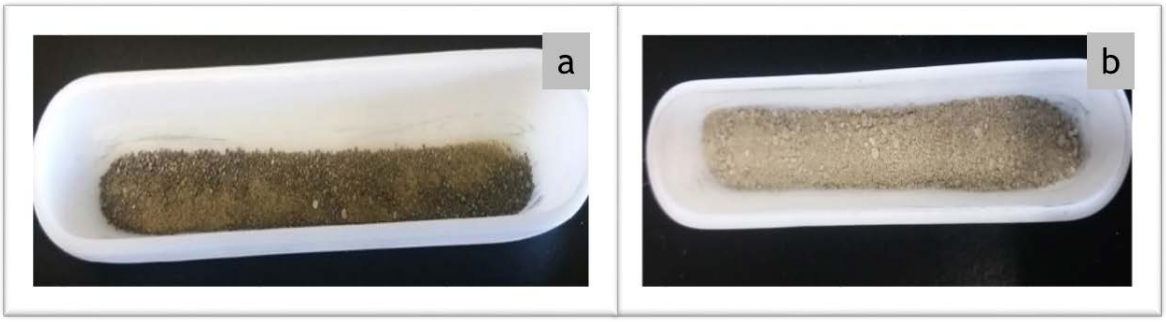

Figure 2:(a) shows the fresh catalyst, (b) shows a 6-months poisoned catalyst, much lighter in color as a result of silica deposition

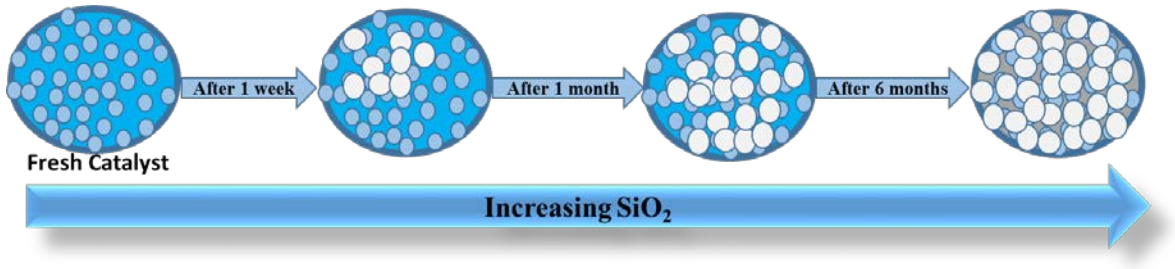

Figure 3: Schematic of the effect of increased SiO_2 addition on the reforming catalyst.

4.2 Characterization

The catalysts were characterized using temperature-programmed reduction (TPR), X-ray diffraction (XRD), N_2 physisorption (BET), SEM/EDS, and FTIR were also utilized. A Cirrus MKS mass spectrometer (MS) connected in-line with a u-tube reactor containing 75.5 mg of catalyst was used for the TPR studies. Prior to running the studies, MS calibration curves were used to obtain ionization factors. The catalyst was placed between two layers of quartz wool to keep it in place inside the reactor. The reactor was then placed inside a Thermoscientific Thermolyne tube furnace and insulated with high temperature glass wool at the top. Alicat Scientific mass flow controllers were used to control the feed gases. Condensation was prevented by wrapping all of the gas feeds and outlets in heating tape prior to entering the MS. The furnace

temperature was controlled using a Eurotherm 3110 PID controller. For the TPR studies, catalysts were pretreated under 50 sccm of helium (UHP, Airgas) for 30 min at 110°C. Catalysts were then cooled to 50°C where the gas flow was switched to 5% H_2/He (50 sccm). The sample was then heated at a ramp rate of 10°/min to 900°C and held for 30 min.

X-ray diffraction patterns were obtained using a Bruker AXS diffractometer using a Cu Kα source at 40 kV and 40 mA. The data were obtained using a (2θ) angular range of 20-80°. The step size was 0.02° and the dwell time was 3 sec for each step.

Brunaur Emmett and Teller (BET) surface area as well as BJH pore volumes and pore diameters were obtained using a Quantachrome Autosorb-IQ. Each experiment was done using 55 mg of catalyst. Pretreatment was done for each sample by placing it in an oven at 120°C for 2 hr prior to loading to remove any moisture. The catalyst was then loaded in a small-bulb 6 mm quartz cell. The sample was backfilled using helium where it was then outgassed under vacuum for approximately 6 hrs. The surface area values were obtained by fitting the data to a BET isotherm in the P/P_0 range of 0.05-0.33 using N_2. The pore volume is reported at P/P_0 of ~1.

A Hitachi S-800 scanning electron microscope equipped with energy dispersive spectroscopy (SEM/EDS) was used to obtain the catalyst images.

A Fischer Thermoscientific Nicolet iS50 FT-IR/DRIFTS with multibounce ATR was used to obtain infrared spectra of the catalysts.

4.3 Catalytic Testing

The catalyst was reduced in a 5% H_2/He mixture at 300°C for 1 hour prior to running the dry reforming reaction experiments. Upon reduction completion, the catalyst was cooled to 200°C under a constant flow of 50 sccm of inert He. After temperature stabilization, carbon dioxide and methane were introduced (both 99.999% pure from Airgas) were then introduced in a 1:1 ratio to the catalyst. The overall gas hourly space velocity was maintained constant at 68,000 h^{-1}. The temperature was then ramped at 10°C/min to 900°C and held for 30 min.

5. RESULTS AND DISCUSSION

Two different catalysts, a high temperature one with 1.34%Ni and 1.00%Mg and a low temperature one with 0.16%Pt added to the Ni and Mg were synthesized on ceria zirconia oxide

support ($Ce_{0.6}Zr_{0.4}$)O_2. The catalysts were poisoned using Ludox ® to study the effect of siloxane poisoning. Ludox®, which is a silica colloidal suspension, was chosen to poison the catalyst and simulate the effects of the catalyst being subjected to VMS present in LFG. The theory behind this is that siloxanes are so damaging to equipment because they irreversibly decompose to silica. Therefore, although the siloxanes are the starting compounds, however the damage actually results from the silica, hence why the catalyst was poisoned with silica to simulate decomposed VMS.

Three different poisoning amounts were chosen, 1 week, 1 month and 6 months to study the effects of accelerated deactivation. The amounts were chosen based on several assumptions including a plant that operates on a 24/7 basis with a flowrate of 4248 m^3/hr. The density of the catalyst was taken to be 1704.5 kg/m^3. A survey of available literature showed a varying range of approximations for amount of siloxanes present in LFG since it depends on size and content of waste in the landfill. With that in mind, the concentration of siloxanes in the feed was assumed to be 5mg/m^3 ultimately equivalent to ~2 mg Si/m^3 which is in the mid-range of the literature values. This Si amount would then result in an equivalent SiO_2 amount of ~4 mg SiO_2/m^3. A gas hourly space velocity (GHSV) of 68,000 h^{-1} was utilized for the lab experiments. Sample calculations for Silica % weight gain based on the assumptions is provided in the supporting information; the results along with the nomenclature that will be used for the poisoned catalysts is provided in Table 7:

Table 7: Mass gain of silica

Catalyst Composition (Fresh)	**Sample**	**Nomenclature**	**Mass Gain SiO_2**
1.3 wt% Ni-1.0 wt% Mg/$Ce_{0.6}Zr_{0.4}O_2$	1 week NiMg	1W-NiMg	1.5%
	1 month NiMg	1M-NiMg	11.9%
	6 month NiMg	6M-NiMg	65.7%
0.16 wt% Pt-1.3 wt% Ni-1.0 wt% Mg/$Ce_{0.6}Zr_{0.4}O_2$	1 week Pt	1W-Pt	1.1%
	1 month Pt	1M-Pt	10.5%

	6 month Pt	6M-Pt	61.9%

5.1 Characterization

5.1.1 TPR

The reducibility of the catalyst was determined through temperature programmed reduction experiments (TPR) and are provided in Figures 4 and 6. Catalyst reduction is measured by tracking the formation of water shown by mass to charge ratio (m/z=18) from the output of the mass spectrometer. Reduction temperature has been identified to be directly related to activity with lower temperatures indicating higher activity as previously reported by this group (Elsayed *et al* 2015). All catalysts had a similar reduction profile with an initial peak indicating the formation of water then a tail as shown in Figures 4 and 5. Overall, the Pt catalysts (fresh and poisoned) had lower reduction temperatures compared with the NiMg only catalysts. The fresh Pt catalyst displayed a reduction temperature of 248 °C as reported in a previous study done by this group (Elsayed *et al* 2015). Addition of poisoning caused an increase in reduction temperature where 1W-Pt had a reduction temperature of 304 °C. The 1M-Pt had a reduction temperature of 311 °C. The trend continued where 6M-Pt reached a high reduction temperature of 315 °C. The same trend was present in the NiMg only catalyst. Increasing the poisoning amount caused an increase in the reduction temperature from 382°C for the fresh catalyst to a high of 546 °C for the 6M-NiMg catalyst.

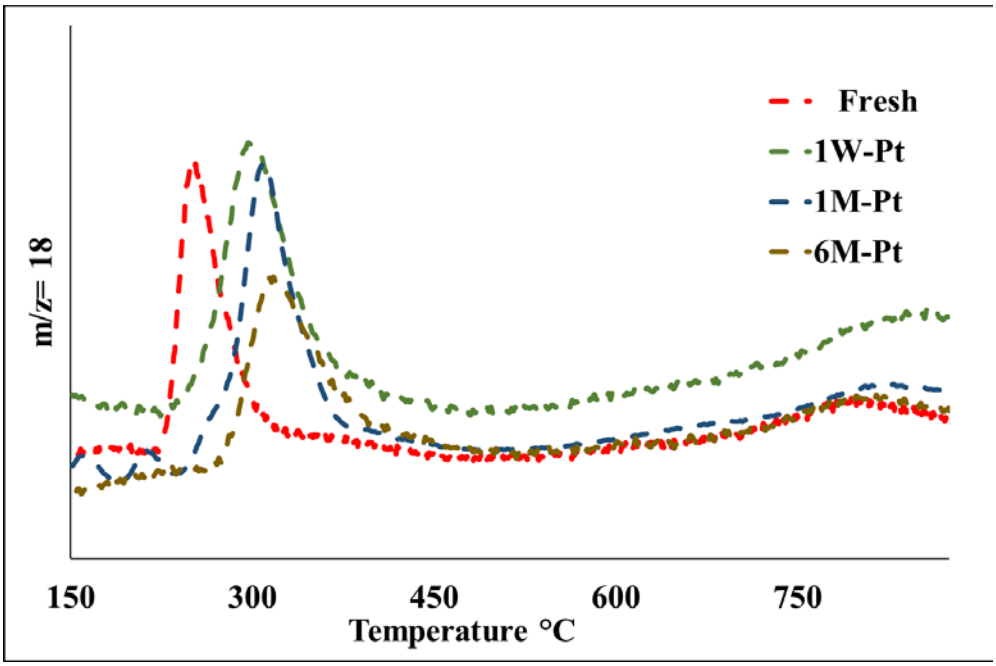

Figure 4: Temperature-programmed reduction (TPR) profiles as represented by water formation (m/z 18), (a) TPR of Pt catalysts

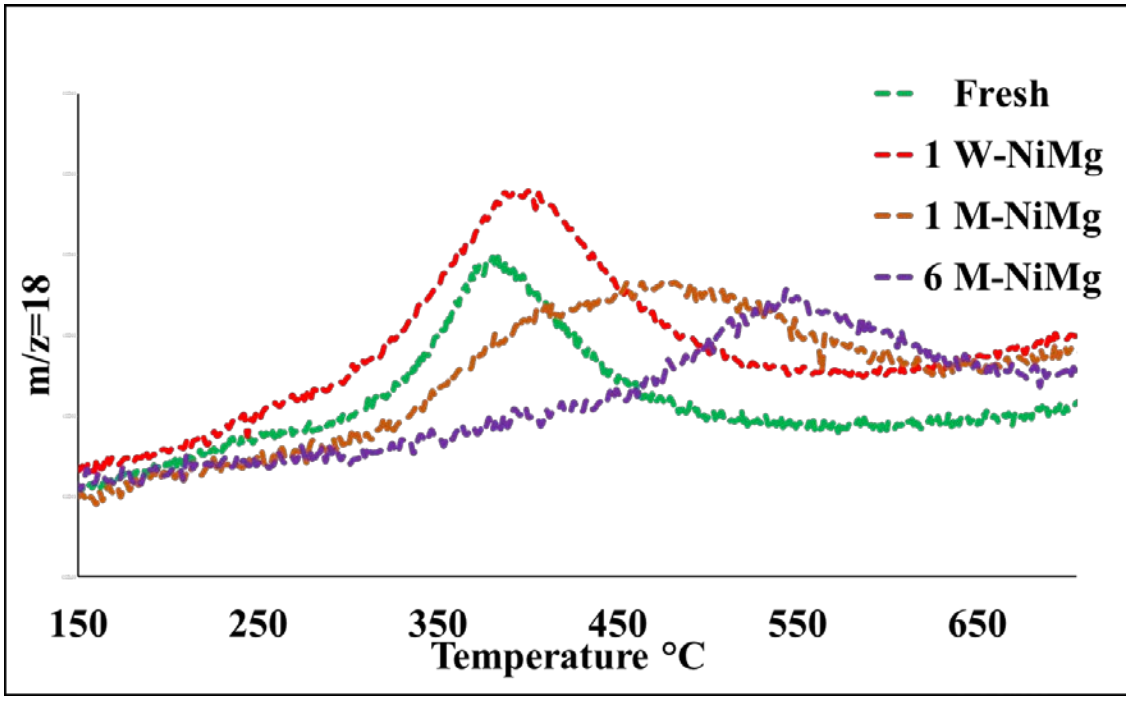

Figure 5: Temperature-programmed reduction (TPR) profiles as represented by water formation (m/z 18), TPR of NiMg only catalysts.

5.1.2 BET Surface Area

Brunauer-Emmett-Teller (BET) surface areas for all the catalysts have been obtained along with pore volumes and pore diameters and are presented in Table 8. It can be seen that the calcination temperature post poisoning had a significant effect on the surface area and bulk properties of the high temperature catalyst. It can be seen that the 6M-NiMg catalyst calcined at 600 °C had a surface area of 73.8 m^2/g whereas the same catalyst calcined at 800°C had an average surface area of 28.2 m^2/g. The same trend was shown for the 1M-NiMg catalysts where the 800°C calcined catalyst had a lower surface area compared to the 600 °C calcined catalyst. The only exception was the 1W-NiMg catalyst at 800 °C which had a surface area of 35.0 m^2/g whereas the 600 °C calcined catalyst had a surface are of 27 m^2/g, however that is within experimental error. The decrease in surface area with silica loading indicates pore shrinkage and blockage which adversely affects the activity of the catalyst since a higher surface area is desirable. This phenomenon was similar to previously published works which also observed a decrease in surface area with increased poisoning.

Table 8: Surface areas and bulk properties

	SA (m^2/g)	**PV (cc/g)**	**PD (nm)**
Fresh Pt*	31	0.07	11.6
1W-Pt	31.5	0.072	9.5
1M-Pt	34.4	0.080	7.2
6M-Pt	59.1	0.120	6.4
NiMg only Calcined at 600°C			
Fresh NiMg	40	0.1	11.4
1W-NiMg	27.0	0.06	11.4
1M-NiMg	36.3	0.087	11.4
6M-NiMg	73.8	0.13	5.2
NiMg only Calcined at 800°C			

Fresh NiMg*	40	0.1	11.4
1W-NiMg	35.0	0.1	11.3
1M-NiMg	28.9	0.07	7.2
6M-NiMg	22.9/33.5	0.06/0.08	8.2/8.2

***From a previous study (Elsayed *et al* 2015)**

Ludox SA: ~220m^2/g

5.1.3 SEM/EDS

Scanning electron microscopy coupled with energy dispersive spectroscopy (SEM/EDS) was done to visually see the differences between the fresh and poisoned catalysts as well as confirm the species present in the catalyst system. All images were taken at 16.0 kV and 3000 magnification. Figure 6(a) shows the fresh 0.16Pt catalyst and it can be seen that there is no silica on the surface of the catalyst. On the other hand, Figure 6(b) shows the 6M-Pt catalyst and the presence of silica is evident by the bright white regions compared to the fresh catalyst. A similar observation was seen in the fresh NiMg shown in Figure 7(a) compared to the 6M-NiMg sample where the evidence of silica was prominent. EDS studies showed the presence of Pt, Ce, Zr, Ni and Mg in the fresh catalyst with percentages within experimental error; the quantitative analyses are summarized in Table 9. Silica was present both for NiMg and 0.16Pt poisoned catalysts as shown in Table 9. This indicates the physical presence of silica and further proves that it has a direct effect in catalyst deactivation as will be discussed in the reaction section. Silica was present in much higher concentrations (40 wt%) in the tested 6M sample compared to 7.94 wt% in the 1M sample (not shown), with no presence in the fresh catalyst as expected.

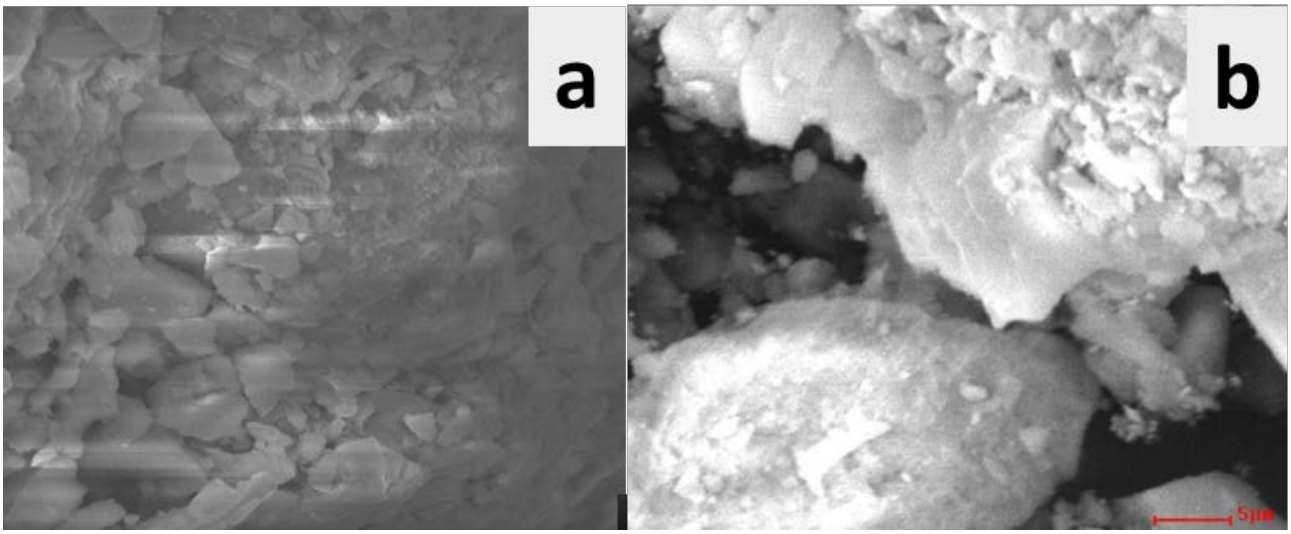

Figure 6: (a) SEM image of fresh 0.16Pt catalyst (b) SEM image of 6M-Pt catalyst

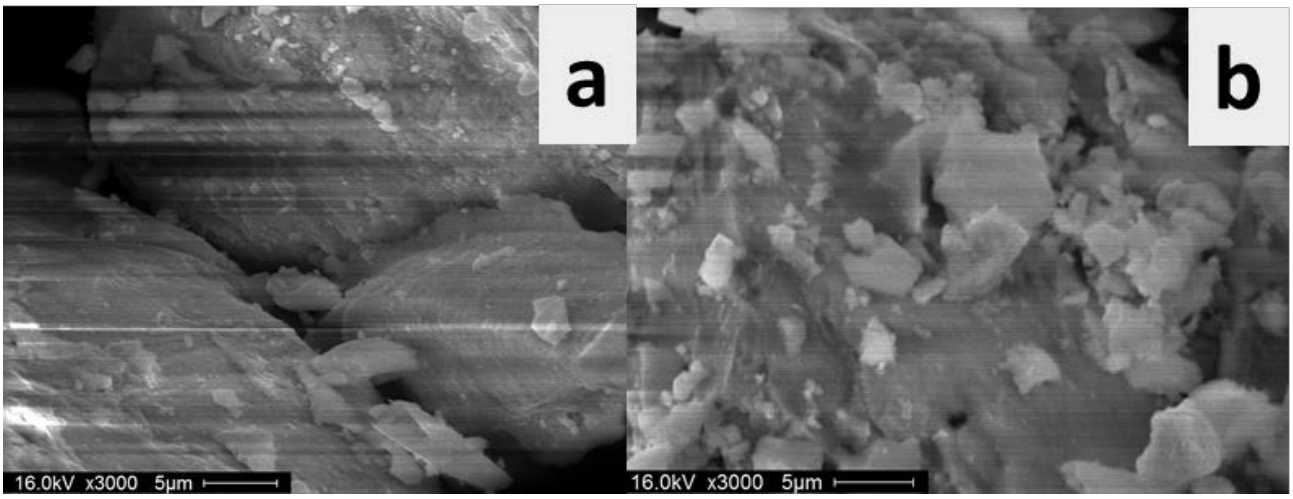

Figure 7: (a) SEM image of fresh NiMg catalyst (b) SEM image of 6M-NiMg catalyst

Table 9: EDS Quantitative Data for Fresh 0.16Pt and NiMg catalysts compared to the 6M-Pt and 6M-NiMgcatalysts

	Fresh Pt		**6M-Pt**	
Element	**Wt%**	**At%**	**Wt%**	**At%**
C	32.4	69.5	20.6	nd
O	11.1	17.8	34.3	57.4
Mg	0.4	0.4	0.00	0.00
Si	nd	nd	39.9	38.0
Pt	nd	nd	5.2	0.7
Ce	41.8	7.7	nd	nd
Ni	3.9	1.7	nd	nd
Zr	10.4	2.9	nd	nd
	Fresh NiMg		**6M-NiMg**	
Element	**Wt%**	**At%**	**Wt%**	**At%**
O	11.6	49.3	23.8	48.1
Si	nd	nd	32.4	37.2
Zr	18.0	13.4	nd	nd
Ce	66.9	32.5	34.1	8.04
Ni	3.3	3.8	9.2	6.1
Mg	0.36	1.02	0.40	0.60

nd= not detected

5.1.4 FT-IR

Fourier Transform infrared spectroscopy (FT-IR) was done on all the catalysts to determine if there are any peak shifts or additions as shown in Figures 8 and 9. It can be seen that addition of silica has changed the peaks in the 700-1250 cm^{-1} range. Both crystalline and amorphous silica have peaks in the same range. This indicates that the catalyst has been poisoned and silica is now present. Peaks in the lower range of 950-1100 cm^{-1} are indicative of stretching vibration of Si-O-Si bonds (Cheng *et al* 2003). These findings are similar to previous findings found in literature (Rasmussen *et al* 2006) who concluded that the catalyst was likely poisoned through a bond formation of a partially oxidized siloxane species to an active Pt site. Similar absorbance peaks were visible for the NiMg only catalyst indicating the presence of silica for the poisoned catalyst that were absent in the unpoisoned catalyst.

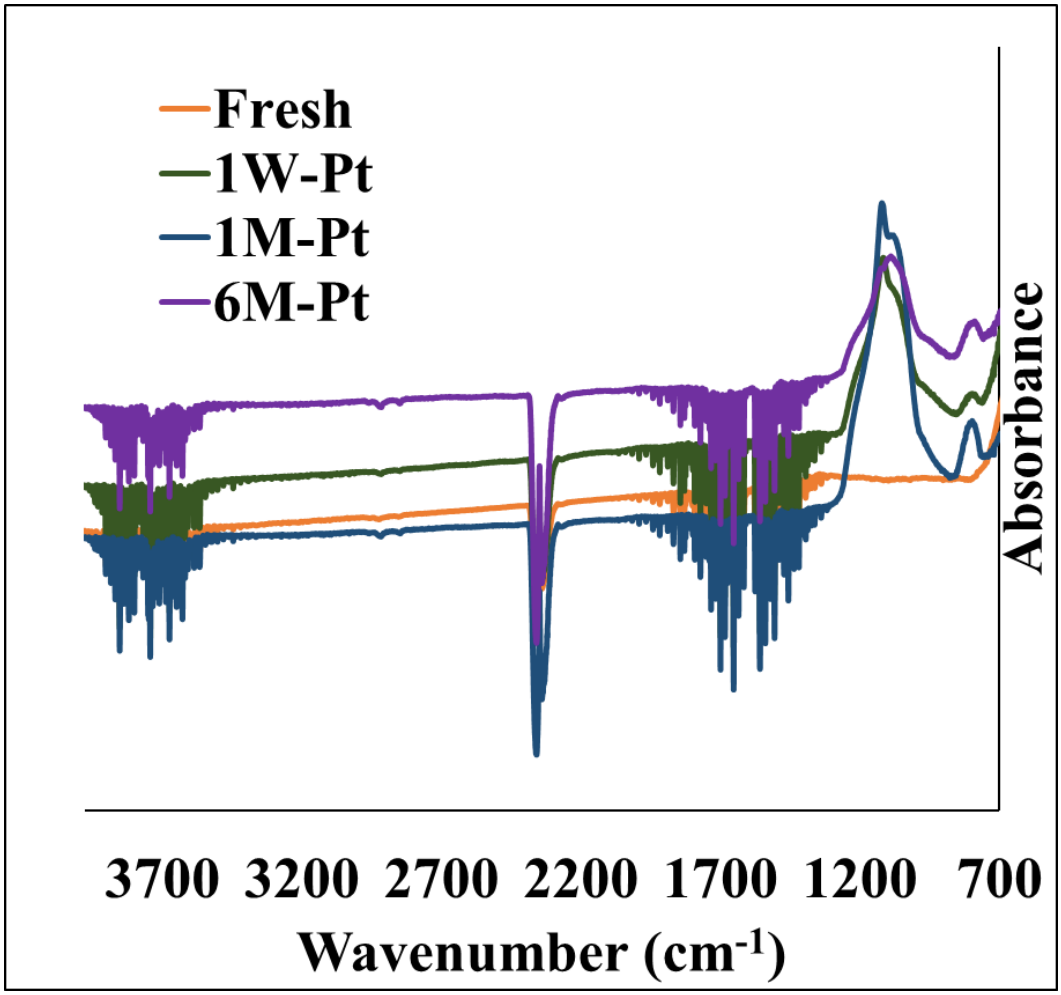

Figure 8: IR spectra of Pt catalysts both poisoned and fresh

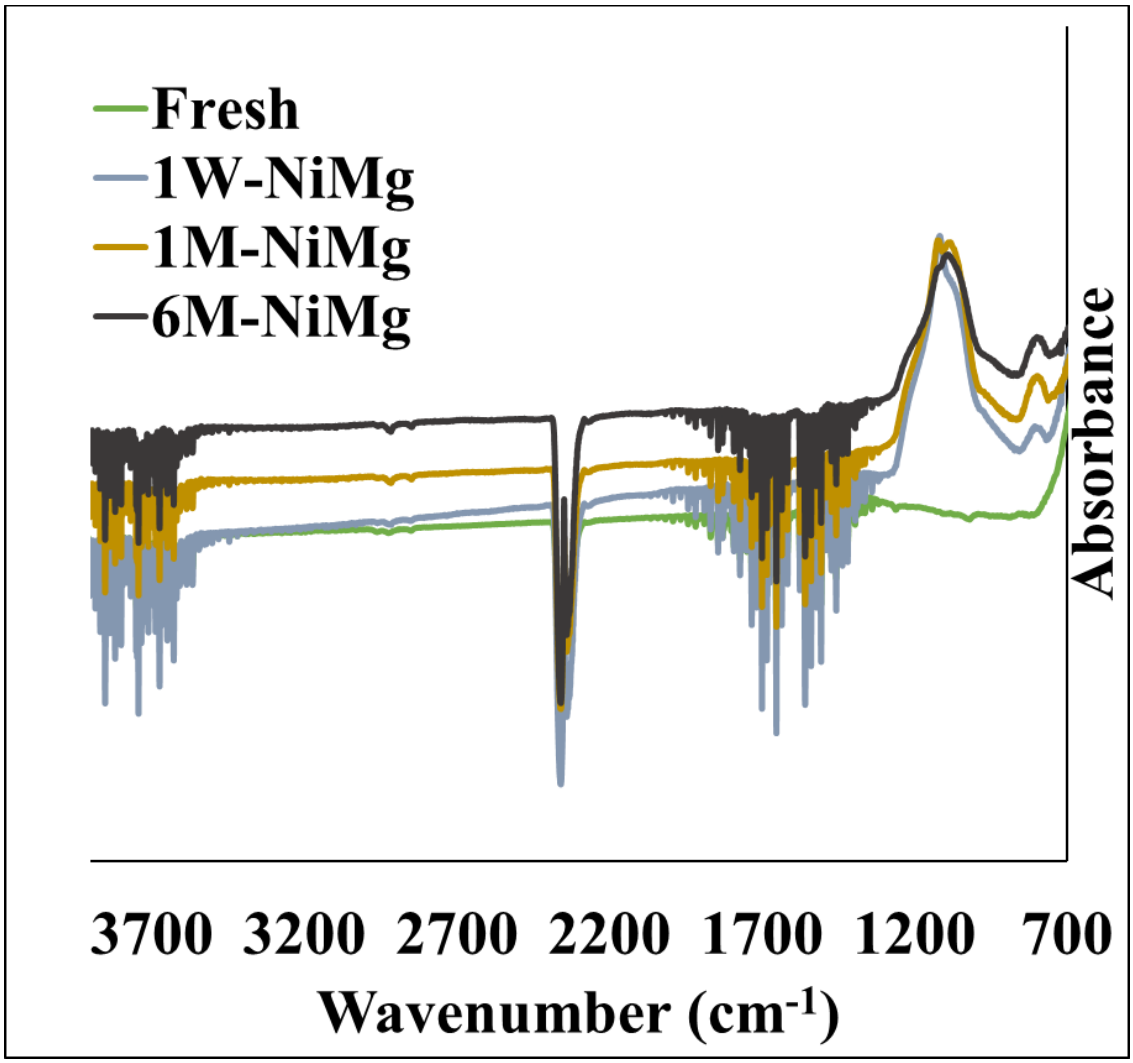

Figure 9: IR spectra of NiMg catalysts both poisoned and fresh

5.1.5 XRD

X-ray diffraction (XRD) patterns are shown in Figures 10 and 11. It is evident that silica has been deposited onto the catalyst even at the smallest amount used. This can be seen by the change in the diffraction pattern at the lower 2theta (20-25°) values as indicated by the arrows showing the broad peak consistent with an amorphous phase, which would like be silica. The first diffraction pattern at the very top shows a fresh, un-poisoned catalyst. It can be seen that only diffraction lines associated with ceria are shown.

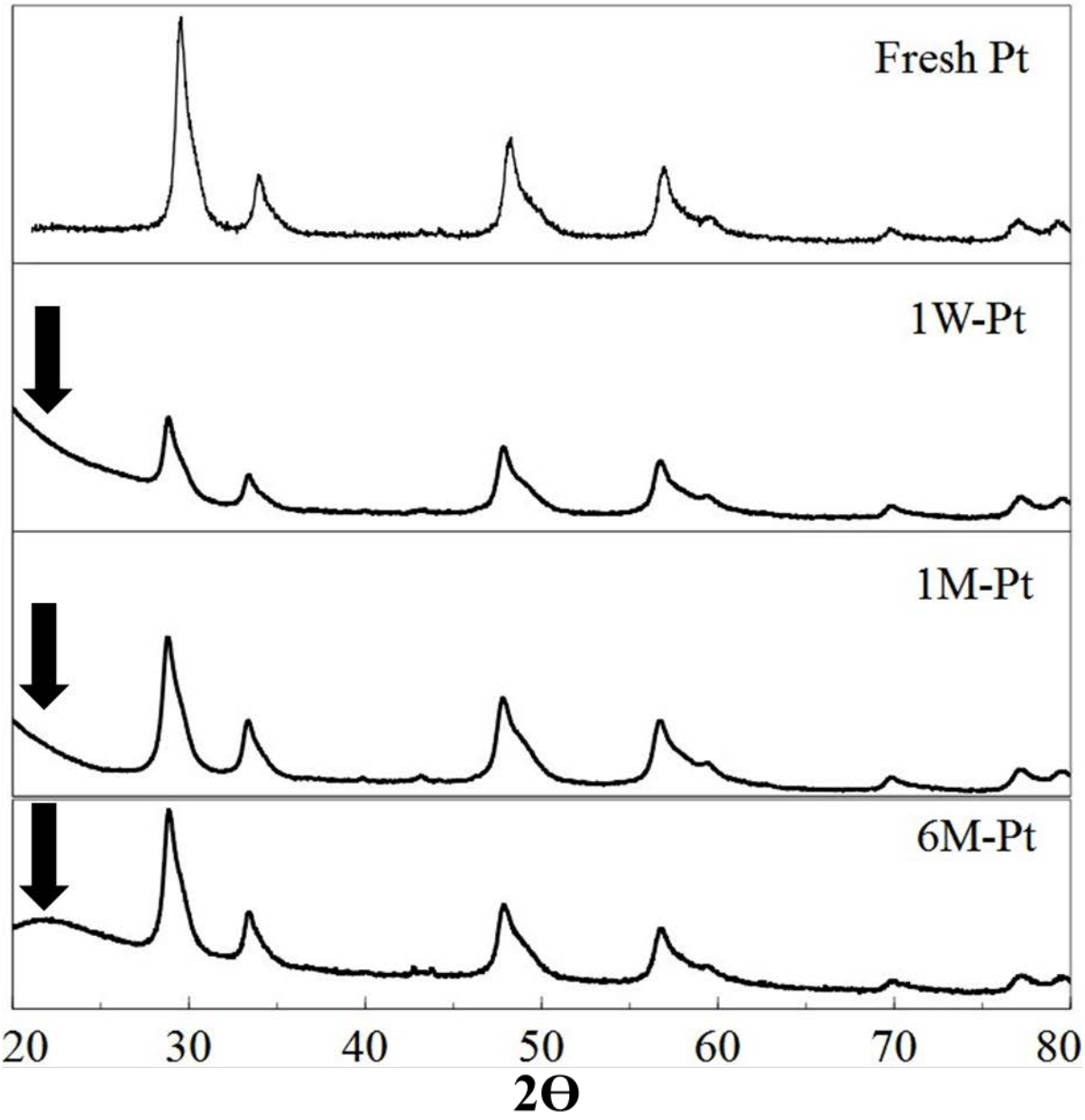

Figure 10: X-ray diffraction patterns of 0.16Pt catalysts both fresh and with different poisoning amounts

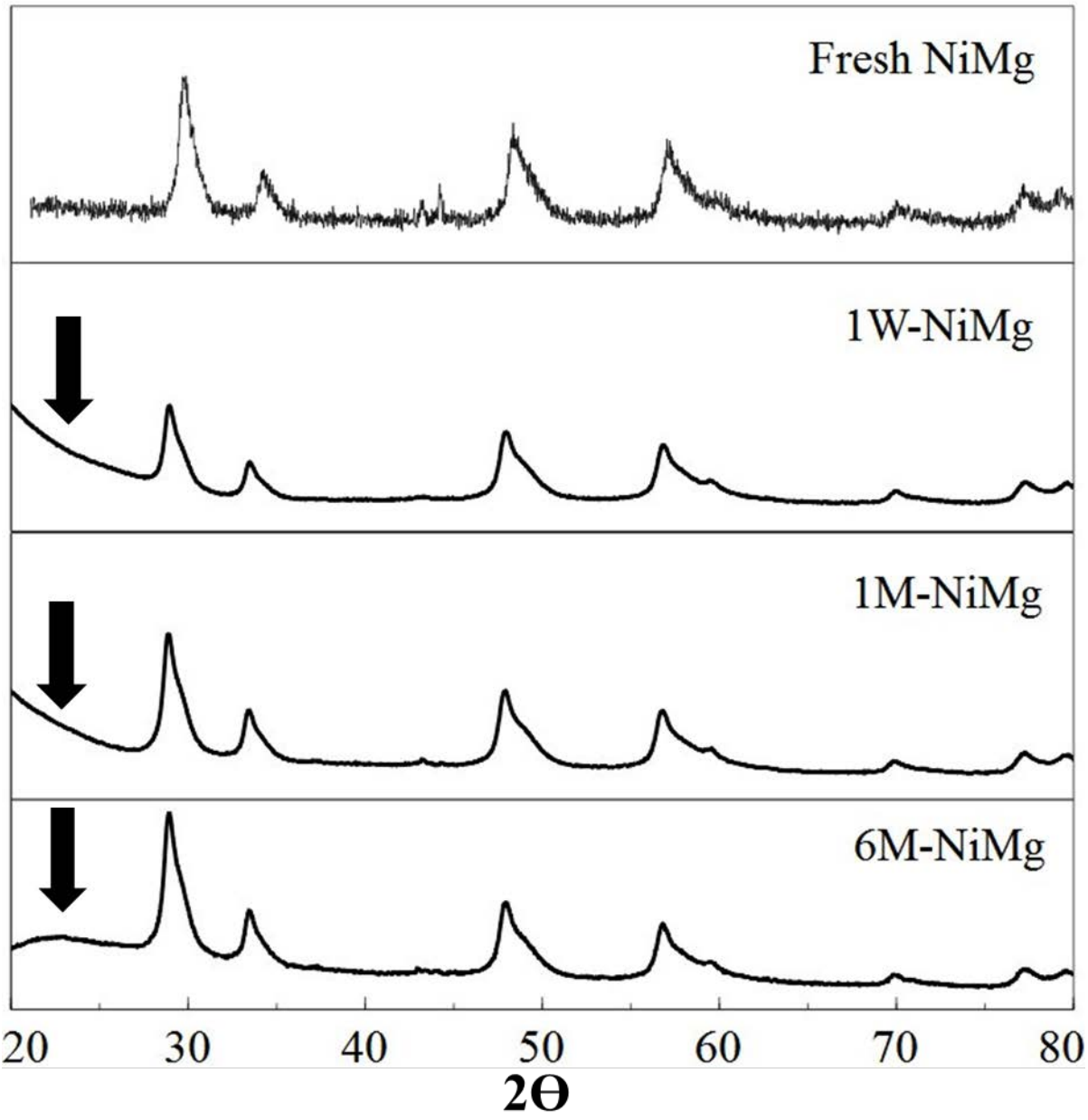

Figure 11: X-ray diffraction patterns of NiMg catalysts both fresh and with different poisoning amounts.

5.2 TP-Dry Reforming

Hydrogen and carbon monoxide production as a function of temperature is shown in Figures 12-15. It is evident that the fresh catalysts (0.16Pt and NiMg) were able to reform methane to produce both H_2 and CO at lower temperatures compared to the poisoned catalysts. Catalytic activity decreased with increased poison amount as evident by the increased temperature at

which H_2 and CO were produced. Table 10 summarizes the findings of temperatures where 10% (X_{10}) and 50% (X_{50}) of both CH_4 and CO_2 were converted to syngas. Addition of even minute amounts of silica as seen in the 1W-Pt catalyst has caused an increase in conversion temperature from 454 to 518 °C for X_{10} CH_4 conversion and from 402 to 503°C for X_{10} CO_2 conversion. Higher poisoning amounts have successively increased the conversion temperature to reach a maximum of 586.8 °C for X_{10} CH_4 conversion for the 6M-Pt catalyst and 566 °C for X_{10} CO_2 conversion for the same catalyst. The syngas ratio (at 450 °C) also suffered with the addition of poison. For the low temperature catalyst, 0.16Pt, the ratio decreased from 0.30 for the fresh catalyst to 0.22 for 1W-Pt sample and continued to decrease ultimately reaching 0.11 for 6M-Pt catalyst. Ideally, higher syngas ratios near 2:1 at a minimum are required for chemical processes such as methanol synthesis and Fischer Tropsch Synthesis (FTS). Similar observations were seen for the NiMg only catalyst where the temperature increased from 762.3 to 809.8 °C for the X_{10} of CH_4 for the 1W-NiMg catalyst and reached 841.8°C for 1M-NiMg. Furthermore, addition of silica has caused the 50% methane (X_{50}) conversion and in the case of 6M-NiMg, the X_{10} conversion to be unreached thereby making the catalyst essentially unusable. The syngas ratios also decreased with increased poisoning amounts as observed in the low temperature catalyst. At 800°C, the fresh catalyst had a syngas ratio of 0.31 which decreased to 0.13 for the 1W-NiMg catalyst and reaching 0.09 for 1M-NiMg sample. There was no detectable H_2 or CO produced at 6M-NiMg catalyst which correlates to the lack of reactant conversion. It is important to note that the tested NiMg catalyst calcined at 800 °C had a higher reduction temperature compared to the 600°C-calcined catalyst indicating that the catalyst will be less active; both TPR profiles are included in the supporting information. Therefore, reaction data was determined to be unnecessary for the higher temperature calcined catalyst. From the previous reaction results, it can be seen that the change in temperatures is comparable for both CH_4 and CO_2 conversion which shows that silica is unselective to different surfaces. Furthermore the addition of small amounts of silica in the 1W-Pt and 1W-NiMg likely results in monolayer deposition versus multiple layers in the 1M-Pt, 1M-NiMg as well as 6M-Pt and 6M-NiMg; which explains the non-linearity in conversion temperature with increased poisoning.

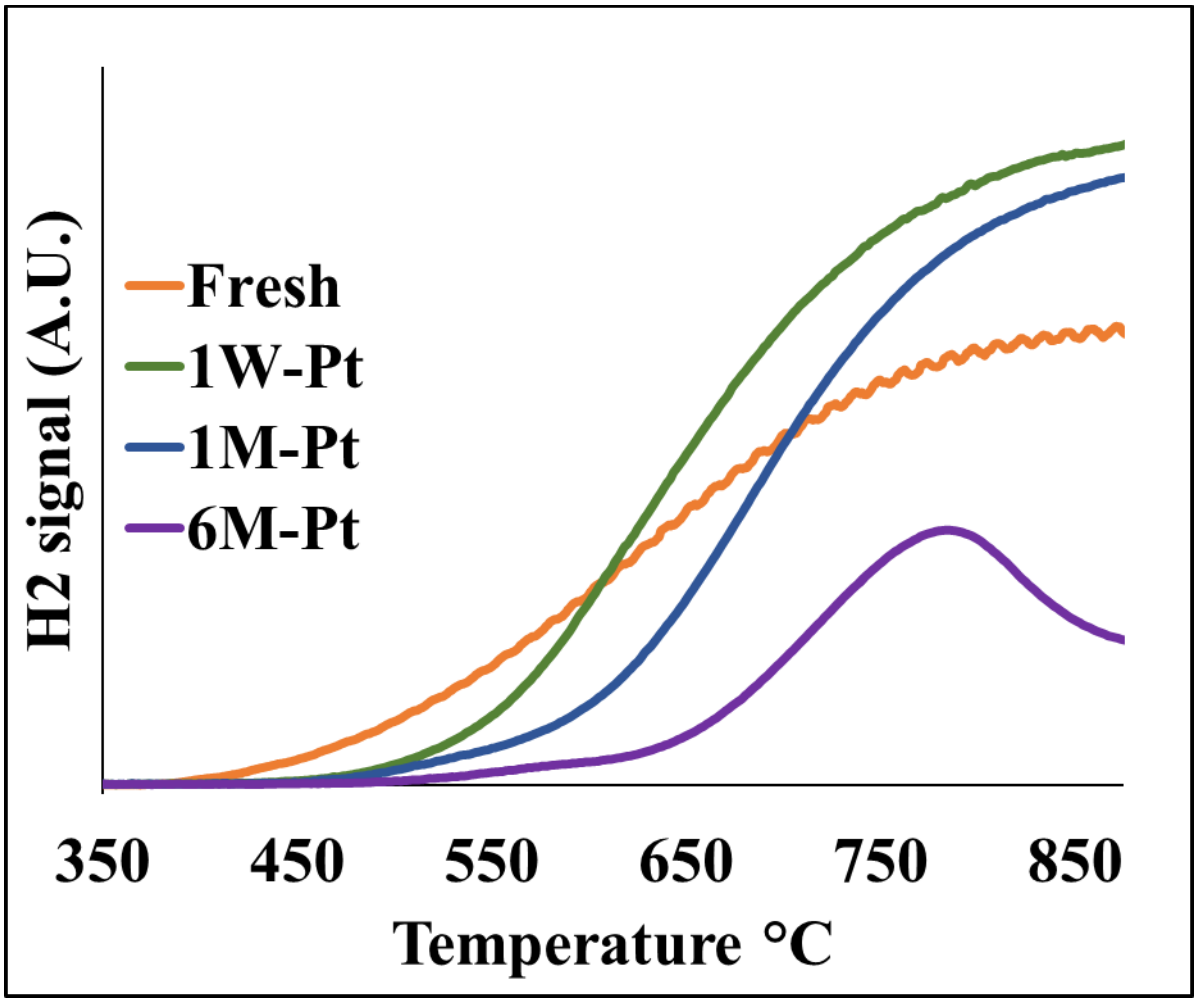

Figure 12: Hydrogen formation over Pt both fresh and poisoned

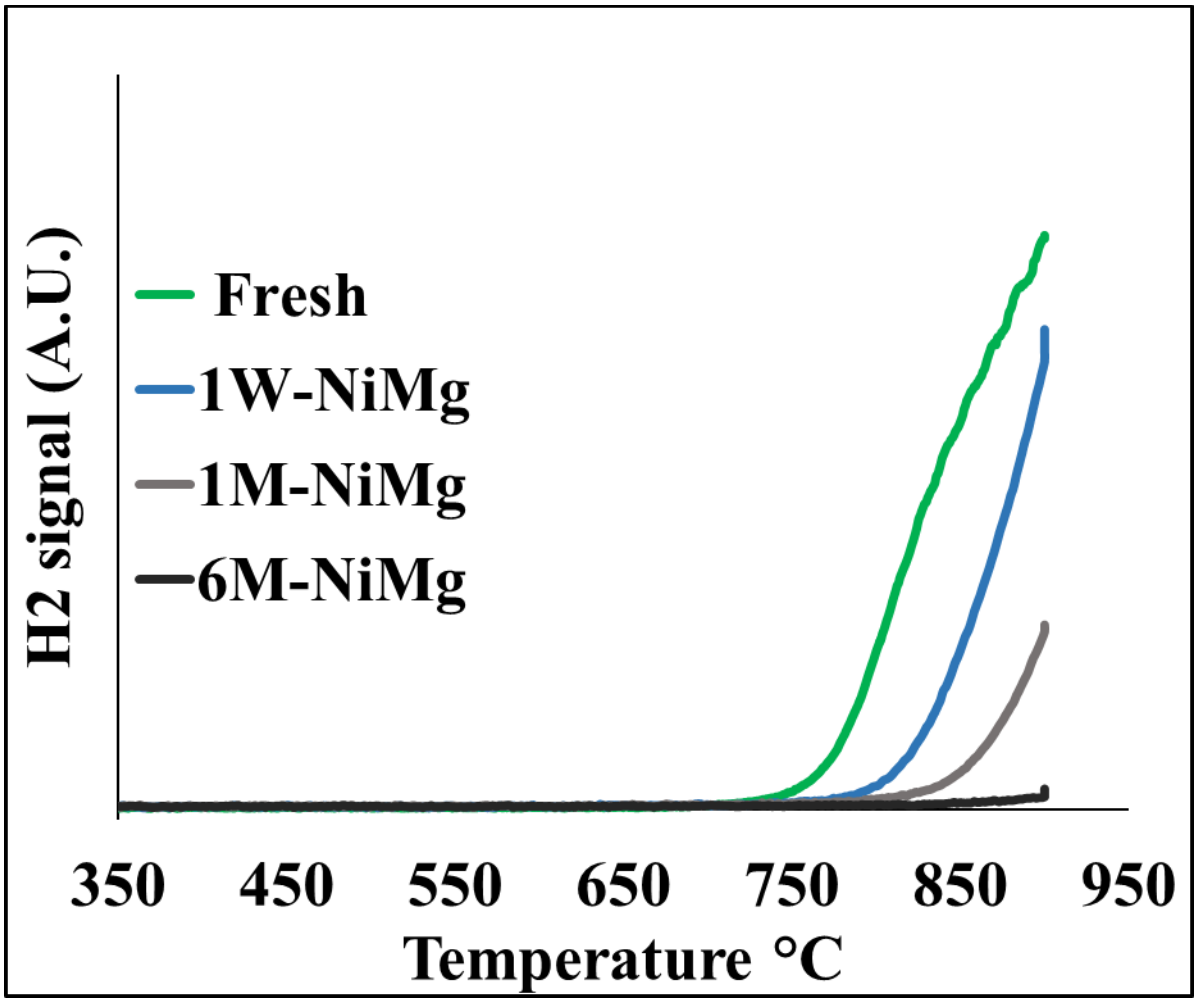

Figure 13: Hydrogen formation over NiMg catalysts both fresh and poisoned with respect to temperature.

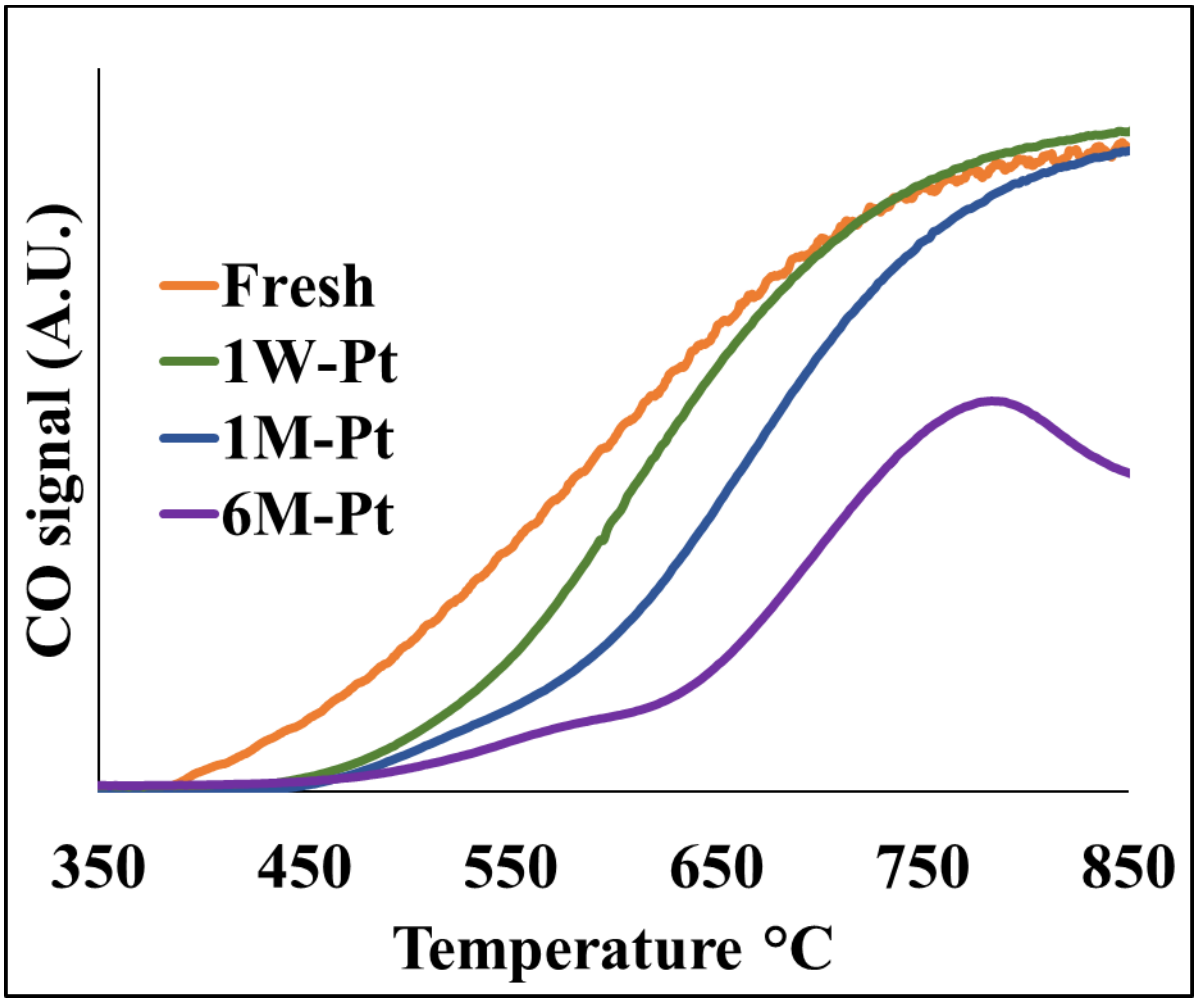

Figure 14: Carbon monoxide formation over fresh and poisoned Pt catalysts with respect to temperature.

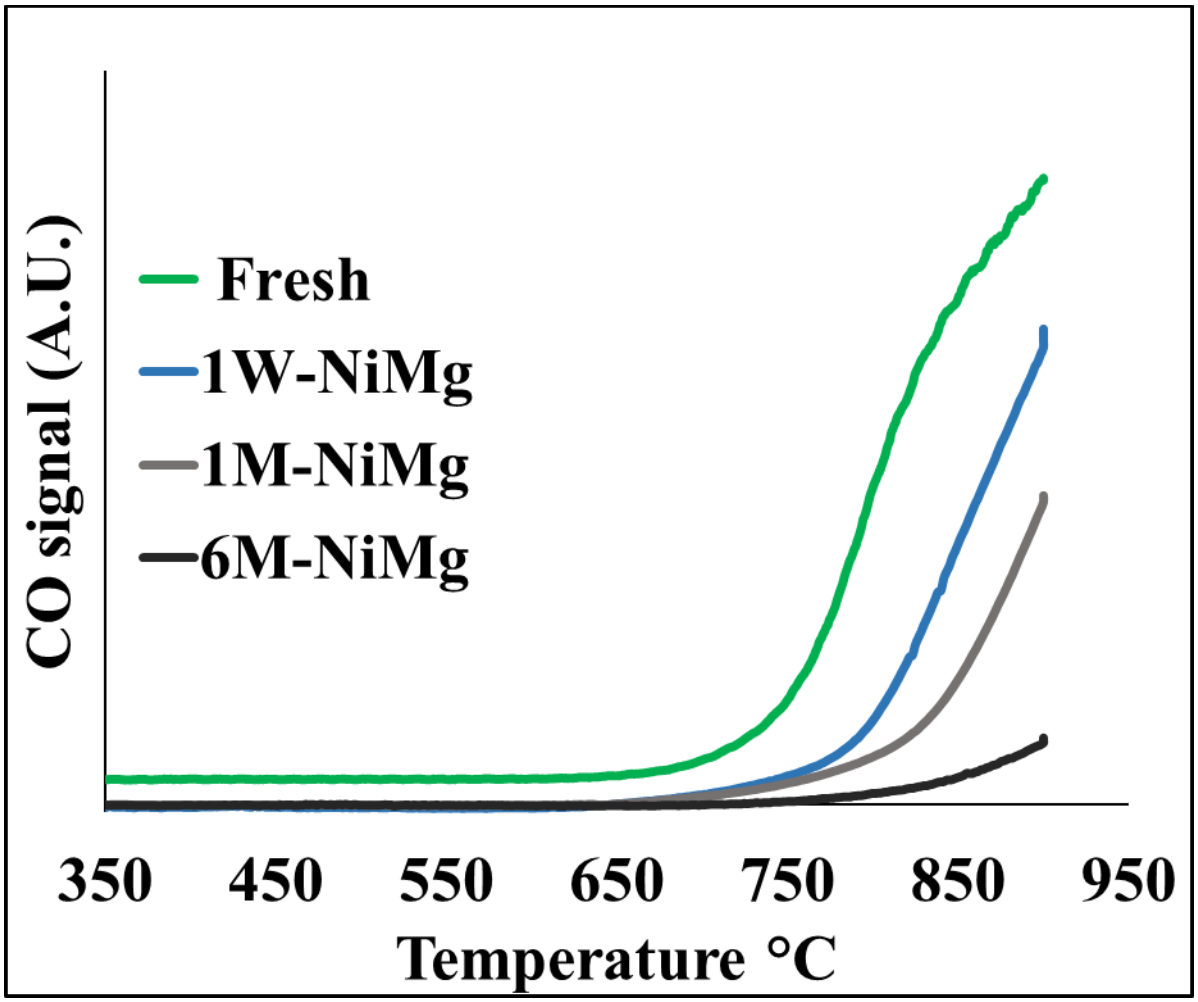

Figure 15: Carbon monoxide formation over fresh and poisoned NiMg catalysts with respect to temperature

Table 10: Methane and Carbon Dioxide 10% (X_{10}) and 50% (X_{50}) conversion temperatures

Pt Catalysts	CH_4 Conversion Temperature °C		CO_2 Conversion Temperature °C		H_2:CO (@450°C)
	X_{10}	X_{50}	X_{10}	X_{50}	
Fresh*	454	603	432	578	0.30
1W-Pt	518	630	503	613	0.22
1M-Pt	535	675	510	657	0.20
6M-Pt	587	752	566	726	0.11
NiMg Catalysts	CH_4 Conversion Temperature °C		CO_2 Conversion Temperature °C		H_2:CO (@800°C)
	X_{10}	X_{50}	X_{10}	X_{50}	
Fresh*	762	848	742	813	0.31
1W-NiMg	810	900	790	875	0.13
1M-NiMg	842	nr	827	900	0.09
6M-NiMg	nr	nr	900	nr	n/a

***From a previous study (Elsayed *et al* 2015)**

-nr: Not reached

n/a: not applicable since there was no reactant conversion

6. ADSORPTION MODELING

6.1. Conditions and Assumptions

The adsorption simulation studies were done using the Transport of Diluted Species in Porous Media package in COMSOL® Multiphysics 5.2a. The model geometry consists of a 3-dimensional cylinder, which represents the adsorbent packing within the bed. There is an inlet set on one face and an outlet set on the other, assuming no radial flux of any species through the pipe walls. Figure

16 shows picture of the model produced in COMSOL®. The study simulated 500 days of clean up in 1 day increments. Gas flow rate was assumed to be 2500 SCFM because it is the average flow of LFG collected according to the LMOP database (EPA 2016d). Atmospheric pressure and a temperature of 25°C were chosen since literature data is given around these conditions and they are reasonable for the industrial scale process (Boulinguiez and Le Cloirec 2010, Nam *et al* 2013, Oshita *et al* 2010, Schweigkofler and Niessner 2001, Sigot *et al* 2014). Low pressure was allowed to be used for schedule 40 piping for the adsorption beds. The velocity through the bed was kept close to values used in experiments from literature (~0.5 m/s) (Oshita *et al* 2010, Schweigkofler and Niessner 2001, Sigot *et al* 2014) by using 10 pipes with a 2-ft diameter. The model gas was comprised of mostly nitrogen and LFG equivalent levels of a single siloxane, L2. This was done for multiple reasons, one being that literature experiments are done using nitrogen as the carrier gas (Oshita *et al* 2010, Schweigkofler and Niessner 2001, Sigot *et al* 2014). It is not necessary to model CH_4 and CO_2 (model LFG) as the carrier because they do not significantly adsorb. CH_4 losses have been reported to be around 2-4% for pressure swing adsorption (PSA) (Sun *et al* 2015). This means it is safe to assume the carrier gas plays no role in the adsorption. Only L2 was chosen to model because larger siloxanes have been shown to break down into smaller siloxanes (L2) and the adsorption of L2 has been widely studied (Oshita *et al* 2010, Schweigkofler and Niessner 2001, Sigot *et al* 2014). The properties of the gas stream were found from nitrogen properties because the L2 levels are dilute enough to be neglected.

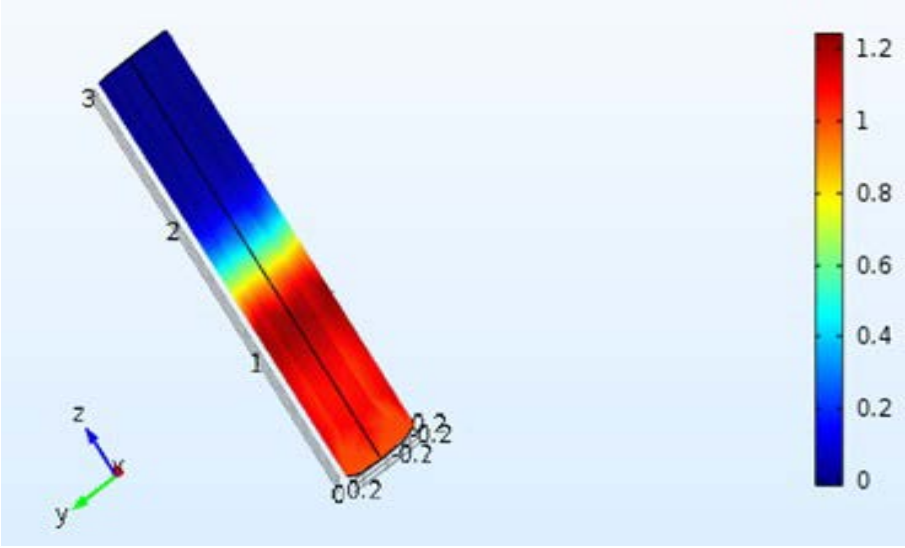

Figure 16: COMSOL® simulation screenshot showing c/c_0 ratio throughout 10 foot adsorption bed

6.2 Parametric Sweep Variables

A parametric sweep to be performed over a range of other variables including bed height, adsorbent, relative humidity, and inlet concentration. These results are able to give data for a wide range of conditions and allows for the sizing and optimization of a viable process for each application of LFG. The bed height was varied between three values: 10, 20, and 30 feet. These heights are all reasonable sizes for the full-scale process and height will affect the bed life and cost. The relative humidity was varied between 0%, 50%, and 100%. Since relative humidity effects the capacity of the adsorbent, its variation allows for optimization of the LFG moisture level for the determination of appropriate pre-treatment steps. Since the concentration of VMS varies greatly between landfills, the initial inlet concentration was assumed to be 10 mg/m^3 which is the average value found in literature with 5 mg/m^3 and 15 mg/m^3 also tested. All of these variables were included in the parametric sweep for two commercially available 4 mm size adsorbents that have been widely studied: activated carbon and silica gel. The parametric sweep in COMSOL® runs calculations for every combination of the variables stated.

6.3 Governing Equations/Correlations

The following equations and correlations were used through COMSOL® to run calculations and/or to calculate data needed as an input to the model.

The material balance used for the adsorption process is shown below in equation (6) (Geankoplis 1993):

$$\epsilon_b \frac{\partial c}{\partial t} + \rho_b \frac{\partial q}{\partial t} = -v \frac{\partial c}{\partial z} + E \frac{\partial^2 c}{\partial z^2} \quad (6)$$

Where ε_b is the bed void fraction, c is the VMS concentration, t is time, ρ_b is the bulk density of the adsorbent, q is the loading of VMS on the adsorbent, v is the superficial velocity, z is the distance along the length of the bed, and E is the axial dispersion coefficient. The concentration at the inlet is equal to the inlet VMS concentration set for the simulation at all times. The concentration and adsorbent loading are both initially 0 and increase with time.

The Freundlich isotherm parameters for the adsorption of L2 on activated carbon and silica gel were obtained from literature (Ricaure-Ortega and Subrenat 2009). The data found was fit to the Langmuir isotherm shown in equation (7), which is the form COMSOL® utilizes for calculations:

$$q = \frac{K_L C_P c}{1+K_L c} \tag{7}$$

The loading of VMS on the adsorbent is q (mol/kg). The concentration of VMS in the gas phase is given by c (mol/m^3). K_L (m^3/mol) and C_p (mol/kg) are the Langmuir parameters, where C_p represents the capacity of the adsorbent. The values used from literature data 0% relative humidity are 412.3 m^3/mol and 1.26 mol/kg for silica gel and 2504 m^3/mol and 2.22 mol/kg for activated carbon.

In order to obtain a relationship between the moisture content and capacity for each adsorbent, literature data was used to develop an equation that gives the adsorption factor (AF) as a function of relative humidity (RH). The adsorption factor is defined as the ratio of the capacity at some relative humidity to the capacity for a dry gas. For activated carbon, graph data from literature (Herdin *et al* 2000) was digitized and fit to a sigmoid equation and regressed to minimize error using equation (8).

$$AF = \frac{3734778}{3758624+e^{26.44(RH)}} \tag{8}$$

Silica gel was also regressed to fit the sigmoid function in equation (9) from available literature data (Schweigkofler and Niessner 2001, Sigot *et al* 2014):

$$AF = \frac{2.65}{1.65+e^{0.046(RH)}} \tag{9}$$

In both equations (8) and (9), AF is a fraction. However, the RH term for activated carbon must be given as a fraction while the RH in the silica gel equation is a percent. AF was used by multiplying its value by the value of the Langmuir capacity term to get the new capacity.

The correlation shown by equation (10) was used to determine the value of the bed void fraction (Ribeiro *et al* 2010):

$$\epsilon_b = 0.373 + 0.917e^{-0.824\left(\frac{D}{d_p}\right)} \tag{10}$$

D is the internal diameter of the bed and d_p is the pellet diameter (chosen as 4 mm).

The pressure drop was calculated through the adsorption bed using the Ergun Equation shown in equation (11) (Fogler 2006) :

$$\frac{\Delta P}{L} = \frac{150\mu(1-\epsilon_b)^2 v}{\epsilon_b^3 d_p^2} + \frac{1.75(1-\epsilon_b)\rho v^2}{\epsilon_b^3 d_p} \tag{11}$$

ΔP is the pressure drop across the length (L) of the bed. μ and ρ are properties of the flowing fluid (nitrogen/L2) and represent viscosity and density, respectively.

6.4 Applications to LFG Purification

The parametric sweep results were used for the three LFG to energy processes identified earlier. Since VMS decompose and damage equipment, each application has its own set of specifications for the maximum amount of VMS allowed in the LFG. One application is the use of LFG for combustion engines, which require the least clean up. The specifications change depending on the engine manufacturing company so the lowest VMS tolerance was selected. For engine applications, the limit of VMS was chosen as 1000 ppb_v (9.4 mg/m^3) (Hill 2014). The second application is the conversion of LFG to liquid fuels using heterogeneous catalysts. Catalysts are damaged by VMS at lower levels than engines, with a tolerance of 100 ppb_v (0.94 mg/m^3)(Hill 2014). The most sensitive application is the use of LFG to generate electricity with fuel cells which has a limit ranging from 10-1000 ppb_v (Papadias *et al* 2012). The lowest tolerance was chosen for this fuel cells to accommodate for the variations in its VMS limit, which is 10 ppb_v (0.094 mg/m^3). Table 1 has the VMS tolerance concentrations for each application. These three limits are used to determine the breakthrough time for each variable combination from the parametric sweep. The breakthrough is defined as the time it takes for the outlet gas stream VMS concentration to reach the limit given by each application. Only breakthrough times of at least 6 months (180 days) are deemed viable for the LFG purification process.

7. RESULTS AND DISCUSSION

7.1 Parametric Sweep

Parametric sweeps were performed using COMSOL® 5.2 for activated carbon and silica gel over three variables each with three different specifications. This gives 54 combinations of variables, which can be applied to three applications for a total of 162 different LFG clean up scenarios.

7.2 Moisture Removal

Because landfills are usually saturated, an appropriate dehumidification process was determined and included in the overall LFG cleanup design/costing. The model results show that at most 50% relative humidity can be tolerated, so this was the target set for the pretreatment step. Many LFG

pretreatments include installation of a refrigeration condenser for moisture removal, which also removes some of the contaminants including siloxanes (Kuhn *et al* 2017, Schweigkofler and Niessner 2001). A temperature of 5 °C was chosen as the target dew point temperature for the cooler because it will remove enough moisture to meet the relative humidity requirement (Schweigkofler and Niessner 2001). This gives a relative humidity of about 30% at the operation temperature of the adsorption beds (25°C).

7.3 Effect of adsorbent

Figure 17 shows the breakthrough time with respect to %RH for both activated carbon and silica gel. Breakthrough time is defined as the time it takes for the outlet VMS concentration to equal the specified application limit. When comparing the ability of activated carbon to silica gel for VMS adsorption, it was found that activated carbon performs much better for every scenario. In some cases, the breakthrough times for activated carbon were an order of magnitude higher. This was expected due to activated carbon's high VMS adsorption capacity compared to silica gel. Although silica gel has a better regeneration ability, it is not enough to overcome its increased cost and decreased capacity. As a result, activated carbon was determined to be the optimum adsorbent for this study. The remaining results are all with respect to activated carbon.

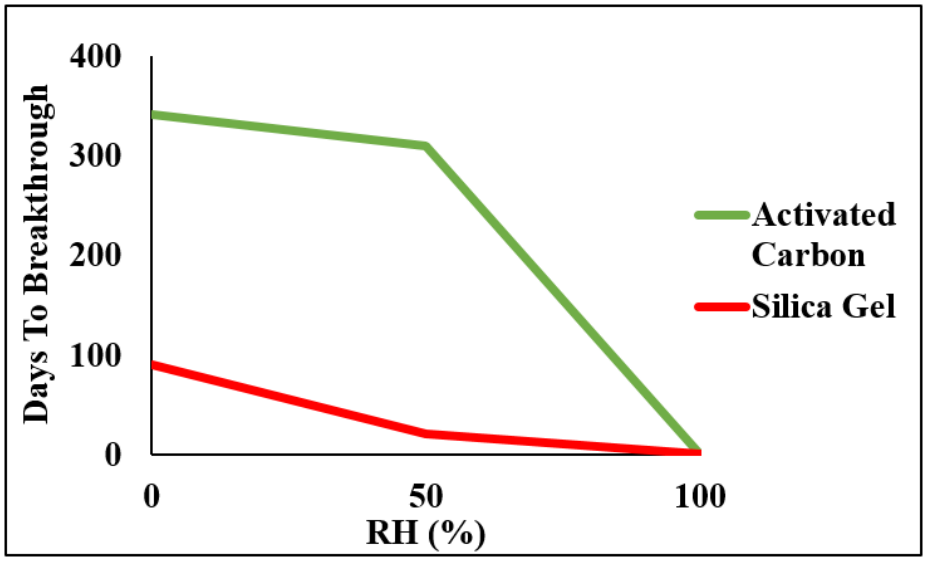

Figure 17: Effect of adsorbent on breakthrough time. Height = 10ft, tolerance = 0.094 mg/m^3, inlet VMS concentration = 5 mg/m^3

7.4 Effect of bed height

The height of the adsorption bed versus the days to breakthrough was analyzed for each application of LFG as shown in Figure 18. For every application, the increased bed height increased the breakthrough time in all cases(Sigot *et al* 2014). One thing to observe is that the height change has different effects on each application. The engine is affected most by height change, then catalysts, and lastly the fuel cells. This trend is likely due to the difference in VMS limits with engines being highest, then catalysts, and fuel cells as the most strict. The lower the VMS limit, the less of a difference a height change will make due to the adsorption isotherm behavior. The concentration plot versus time for adsorption shows relatively no outlet concentration in the beginning, then starts to increase exponentially as the adsorbent is increasingly loaded. At some point in time, the rate of concentration increase will start to slow down, causing the concentration to level off at the capacity of the adsorbent. The breakthrough concentration is very low for fuel cells (0.094 mg/m^3) compared to catalysts (0.94 mg/m^3) and engines (9.4 mg/m^3). This puts the lower VMS limit closer to the point where the concentration rate of change is higher, reducing the effects if having extra adsorbent.

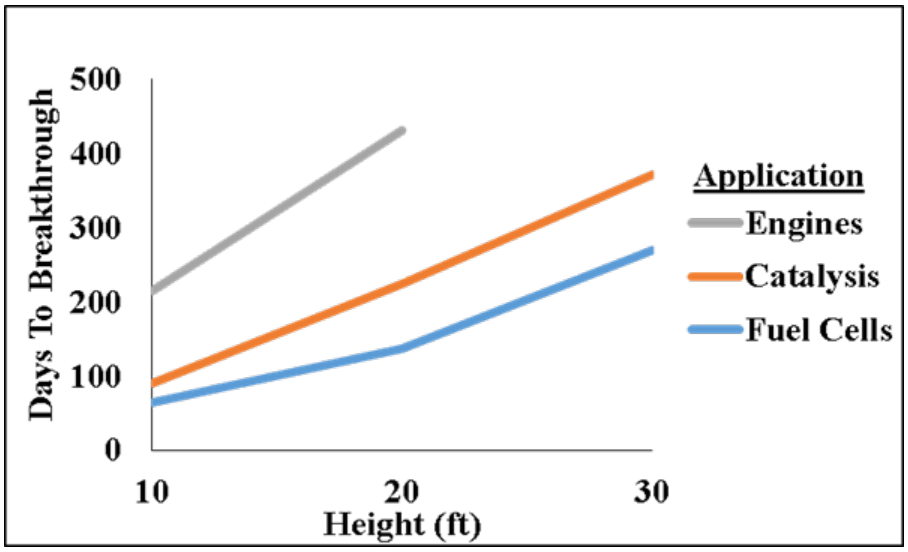

Figure 18: Effect of bed height on breakthrough time. Activated Carbon, inlet VMS concentration = 15 mg/m^3, relative humidity = 0%*

7.5 Effect of VMS Concentration

The effect of inlet concentration on all three applications is shown in Figure 19. In general, as VMS concentration increases, the breakthrough time decreases. This is not surprising since an increased concentration will give more VMS flowing through the bed, causing the bed to adsorb

and breakthrough quicker with the same adsorbent amount. Applications with higher inlet VMS concentrations will require more adsorbent to appropriately remove the contaminant. This is consistent with trends found in literature (Wheless and Pierce 2004). As with the height change, the change in VMS concentration has its largest effect on the engine application, then catalysis, and fuel cells least effected. This happens for the same reason stated above, caused by the difference in application VMS limits and adsorption behavior. Fuel cells tolerate much less amounts of VMS, so even low concentrations will breakthrough quickly and changing them will not have a significant effect. In some cases for engines, the inlet concentration is lower than the 9.4 mg/m^3 limit and no gas purification is needed, such as when the inlet concentration is 5 mg/m^3. This is the reason for the lack of a third data point for 5 mg/m^3 in Figure 19.

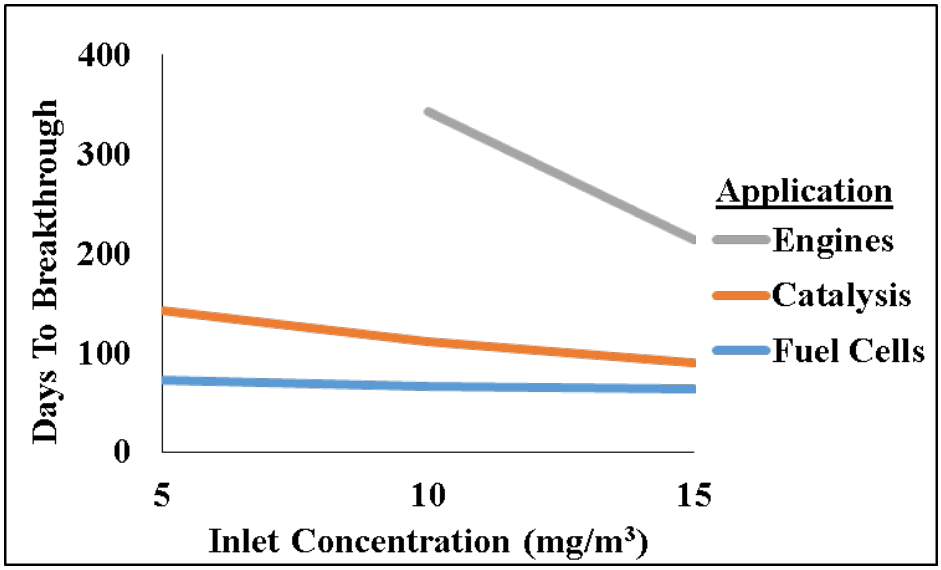

Figure 19: Effect of VMS concentration on breakthrough time. Activated Carbon, Height = 20ft, relative humidity = 0%

7.6 Effect of moisture content

Figure 20 shows the effect of %RH on breakthrough time for all three applications. The moisture content of the inlet gas stream had a negative effect on the breakthrough for every case. Overall, as the relative humidity increases, the breakthrough decreases. This is because there is competition for adsorption sites between the water and VMS, which has been shown to happen in multiple adsorption studies (Herdin *et al* 2000, Ricaure-Ortega and Subrenat 2009, Schweigkofler and Niessner 2001, Sigot *et al* 2014). The data suggests that 100% humidity will lead to virtually no VMS removal in the gas, which is expected due to the study done by Herdin et al (Herdin *et al*

2000). Since LFG is usually saturated, a dehumidification process is so this further shows that it must be dehumidified before VMS removal with activated carbon. Based on these results, the relative humidity should be under 50% to keep the VMS adsorption capacity as high as possible. If it is higher than this, the water will dominate the adsorption.

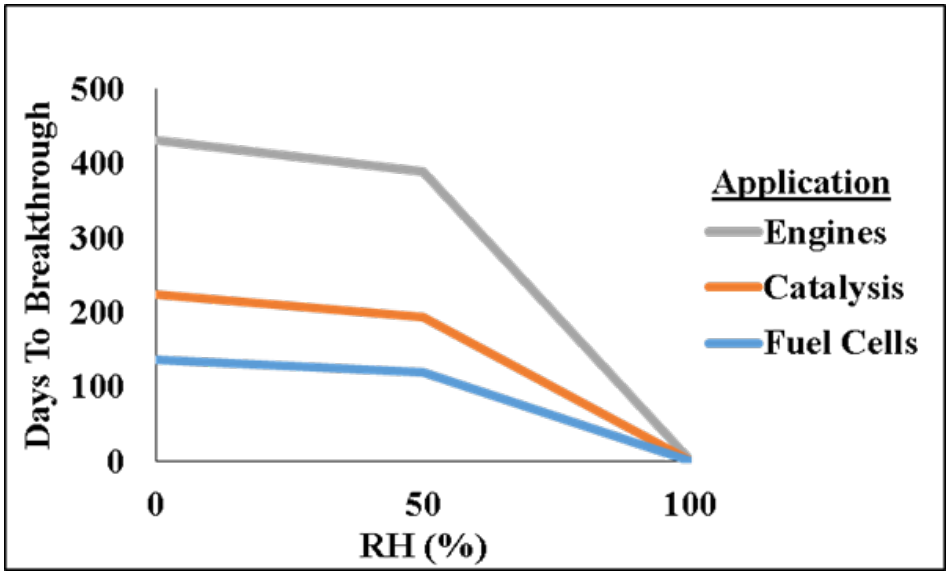

Figure 20: Effect of moisture content on breakthrough time.

7.7 Purification Process Design for the Three LFG Applications

In this study we assumed a desired lifetime of the adsorbent beds to be 6 months (180 days). The parametric sweep results were analyzed to determine which scenarios met this requirement for each LFG application. As stated earlier, activated carbon was found to be better than silica gel and was chosen as the adsorbent. Since 50% relative humidity was the maximum tolerable moisture level, each case with 100% relative humidity was neglected. The results were then narrowed down to only looking at inlet VMS concentrations of 15 mg/m^3. The idea in choosing this is that the process will be able to apply to most other VMS concentrations because it was designed for a "worst-case scenario" situation. From here, size was chosen in order to meet the 180 day breakthrough requirement while keeping the height as low as possible. The breakthrough times for the engine, catalysis, and fuel cell applications are 195, 194, and 217 days, respectively using 10 feet bed height for IC engines, 20 feet for catalysis and 30 feet for fuel cells. Figure 21 shows the ratio of the outlet VMS concentration to the inlet versus time. The final process design results are shown in Table 11.

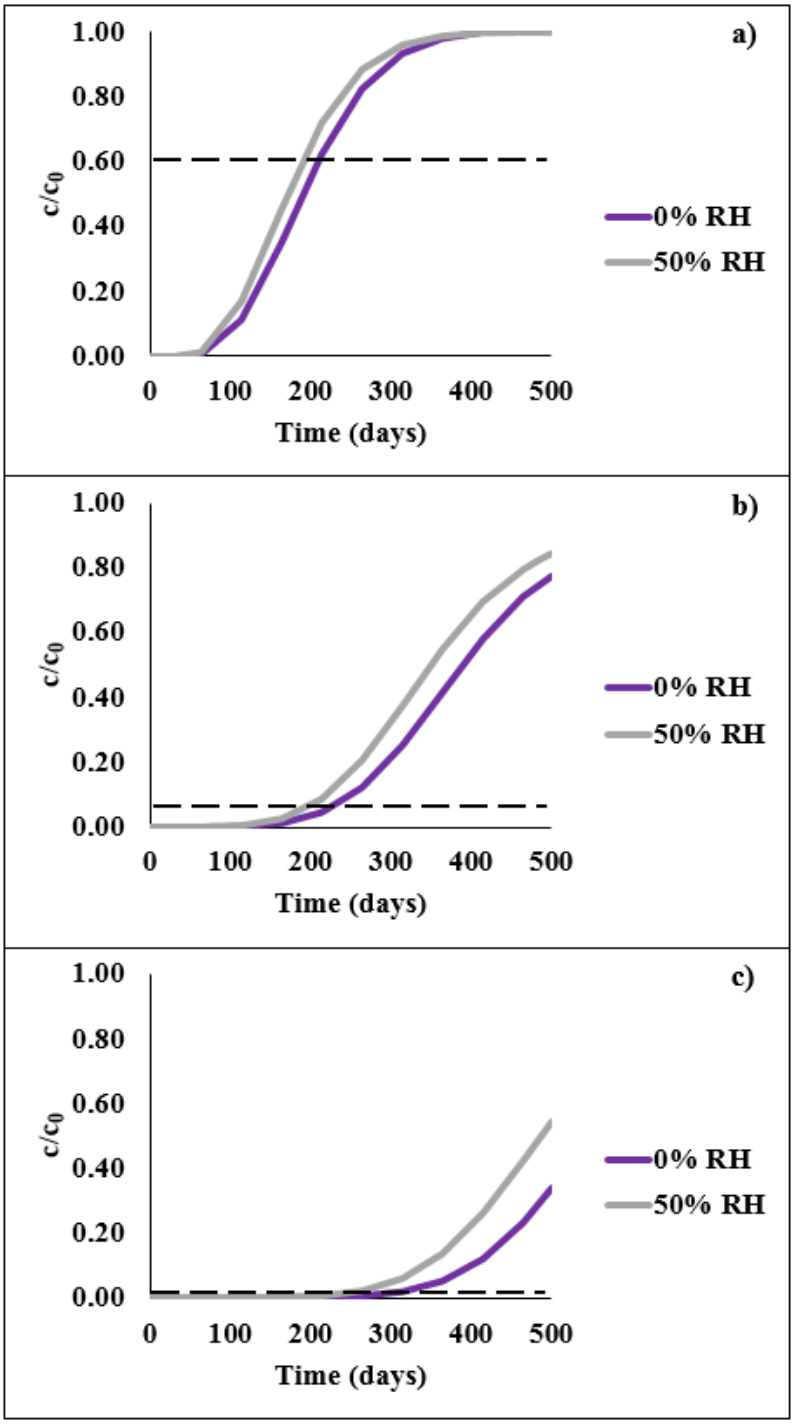

Figure 21: VMS concentration ratio versus time plots for each application's purification process, a) engines, b) catalysis, c) fuel cells. Dashed black lines indicate the breakthrough ratio.

Table 11: Design requirements for three LFG purification processes. All three processes utilize activated carbon, are at 50% relative humidity, and have inlet VMS concentrations of 15 mg/m^3.

Application	VMS Limit (mg/m^3)	Height (ft)	Breakthrough ratio (c/c_0)	Breakthrough time (days)
Engine	9.4	10	0.6	195
Catalysis	0.94	20	0.06	194
Fuel Cell	0.094	30	0.006	217

7.8 Economics of VMS Removal

The costing of the overall process includes a refrigeration condenser, gas blower, and two adsorption beds operating 8400 hours per year to give some scheduled downtime. As shown in Figure 22, two beds were used to allow for constant operation of the LFG processing facility. When one adsorbent bed is used up, the gas is switched to the second bed and the first bed can be disposed and replaced for the next cycle. Since activated carbon does not regenerate well, the processes assume that the adsorbent is thrown away. The bed consists of schedule 40 piping (24 inch diameter) at $76.27 per foot (http://www.pitpipe.com/steel-pipe-prices-inventory.html) and activated carbon bulk priced at $1.20 per pound (http://catalog.adcoa.net/viewitems/activated-charcoal/grade-ac). A headspace of 6 inches was allowed on the top and bottom of the beds. The gas blower was designed with the assumption of a motor efficiency of 90%, a blower efficiency of 70%, and 50 kPa pressure increase to account for pressure drop. The power requirement of the blower is 78.5 kW (Yoon 2016). The purchased cost for the blower was estimated to be $50,000 (Sinnot 2012). The condenser was designed and costed with AspenPlus V8.8 and utilized Freon-12 as the refrigerant. The combined purchased and installed cost is $76,400 with a Freon-12 cost of $1225 per year and electricity consumption of 52 kW. The fixed capital costs (blower, condenser, adsorption beds) were annualized assuming a Lang factor of 4 (to estimate total plant cost), a minimum attractive interest rate of 20%, and a 15 year lifetime. The activated carbon costs were annualized based on the breakthrough time. In September 2016, the electricity costs for industrial facilities in the U.S. was about $0.07 per kWh (EIA 2016a). Labor costing was done

knowing that the gas cleanup is only one step of multiple steps for LFG to energy applications. The pretreatment of the gas is assumed to utilize about half of a single operators time per day, where the operators wage is $35 per hour.

7.9 Hydrogen Sulfide Removal

To develop the comprehensive cost analysis desired, the removal of H_2S must be included. This contaminant has negative effects on equipment because it turns into acid gas, causing corrosion (Urban *et al* 2009). It was not necessary to model a removal process because it has been widely studied and costed. The cost for H_2S removal varies widely depending on application, inlet concentration, and number of processing steps. One study included the cost of H_2S removal assuming 2500 SCFM of LFG and 700 ppm of H_2S. The process was designed to remove H_2S to a level of under 5 ppm (Kent 2016). This concentration is suitable for all applications because it meets the highest removal requirement, which is fuel cells (Papadias *et al* 2012). The costs included from this study were the iron sponge adsorbent (Sulfa-Rite©) and the two parallel adsorption beds. Figure 22 shows everything included in the purification process and cost analysis. The cost of the H_2S adsorbent is $440,000 per year and the two packed beds cost $408,000 (Kent 2016). Table 12 shows the combined costing for VMS and H_2S for each LFG application. Note that the H_2S removal process is kept the same for each application because it assumes the highest required removal level is done. Many landfills do not have the high concentration of H_2S and would not require the removal step (especially for engine applications with a high tolerance). The cost for siloxane removal only is also included in the table. The cost was calculated on a volume of gas processed and amount of contaminant removed basis for each LFG application (Table 12).

Table 12: Total cost of LFG contaminant (H_2S and VMS) removal. The numbers in parenthesis are the costs if VMS is the only contaminant in LFG.

Application	**Cost ($/yr)**	**Cost ($/kg)**	**Cost ($/Nm^3)**
Engine	1,159,000 (370,000)	31.8 (820)	0.031 (0.010)
Catalysis	1,192,000 (402,000)	32.6 (729)	0.032 (0.011)
Fuel Cell	1,217,000 (428,000)	33.3 (768)	0.033 (0.012)

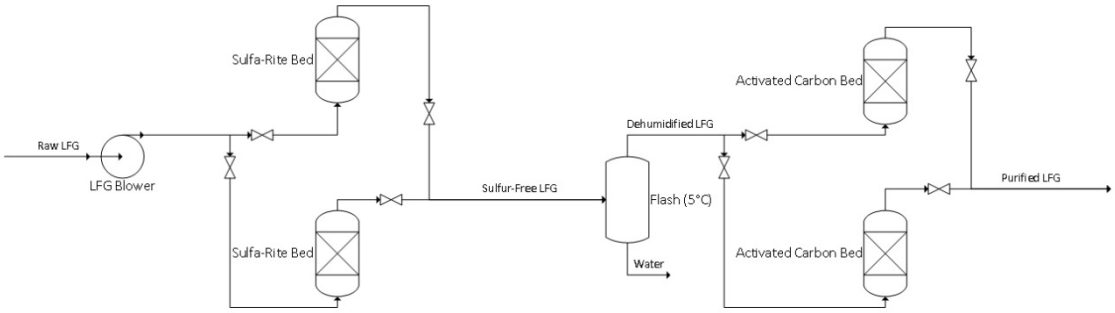

Figure 22: LFG purification process flow diagram

The cost to pretreat LFG is more for applications that have a lower tolerance because they require more adsorbent and larger equipment to remove the contaminant. However, the cost of each application are very similar due to the sulfur removal, which accounts for most of the capital cost and roughly 98.5% of the incoming contaminants by mass. The costs if sulfur is not a contaminant in LFG are included and show a different trend. The cost increases for lower tolerances per year and on a volume of gas process basis, but the cost per kg of contaminant removed is much higher for the highest tolerance (engine application) whereas the other two applications follow the trend of increasing cost with decreasing tolerance. This is because the amount of contaminant being removed is much lower for engines, with only around 81% of the incoming VMS being adsorbed before bed replacement. The catalysis and fuel cell applications have roughly 99% and 100% VMS removal, respectively. Since the amount removed for both catalysts and fuel cells are so close, there is less influence to cause catalysts to cost more than fuel cells per amount removed. In other words, the increased equipment and adsorbent costs for fuel cells outweigh the difference in adsorbed amount. The cost per amount of contaminant removed dramatically increases if H_2S is not included. This is because the VMS is much more dilute in LFG (~1500 ppb_v) than H_2S (700 ppm). When both are included, roughly 100 times as much contaminants are being removed. Dilute concentrations are more costly to remove due to the kinetics and thermodynamics of adsorption at lower concentrations (Kuhn *et al* 2017).

7.10 Economic Impact

In order to understand the economic impact of the purification processes, the costs were compared to the value of LFG and the potential revenues for the three applications. The first method was done by scaling the price of natural gas using the heating value and CH_4 content of LFG. The average heating value is 18,640 kJ/m^3 for LFG and the Henry Hub price of natural gas in December of 2016 was $3.59/MMBTU (Bade Shrestha and Narayanan 2008, EIA 2017). This gives an estimated value of $0.035/$Nm^3$ ($2/MMBTU) for LFG and $1.26E6 per year for 2500 SCFM of LFG. The purification process cost for each application was divided by this value and is reported in Table 3 as a percentage of the potential revenue. The revenues for each application were also estimated for comparison, with engines and fuel cells having their values calculated using electricity values. This electricity would be sold back to the grid at a value equal to the production price of the electricity, which was about $0.033 per kWh in 2015 (EIA 2016b). The efficiencies for engine and fuel cell operation on LFG are 20% and 38% (Bade Shrestha and Narayanan 2008, Spiegel and Preston 2003), corresponding to revenues of $1.23E6 and $2.33E6, respectively. Since the catalysis application involves converting to liquid hydrocarbon fuels, the revenue was adjusted from electricity generation using the ratio of gasoline-gallon equivalent (GGE) values for gasoline and electricity in 2016 (EERE 2016). The annual revenue for the catalysis application is roughly $7.29E6. Each purification cost was divided by its application revenue and is shown as a percentage in Table 3. Again, because the H_2S removal is not always necessary, the cost of only siloxane removal is included. All of the applications can provide more revenue than the cost of cleaning up the LFG. However, if H_2S and siloxane removal is needed for engine applications it seems nearly impractical to remove any impurities. This situation is unlikely because the specified H_2S concentration is an extreme/worst-case level and landfills typically have sulfur concentrations of 0.56 to 280 mg/m^3 which is lower than engines limits (~715-2200 mg/Nm^3) (Kuhn *et al* 2017). Also, due to lack of information, the cost analysis does not include the decreased maintenance and equipment replacement costs for using purified LFG.

Table 13: Cost of purification compared to application revenue and price of LFG. Values in parenthesis are percentages if only siloxanes are removed.

Application	Application Revenue (%)	LFG Price (%)
Engine	94.4 (30.1)	92.1 (29.4)
Catalysis	16.3 (5.51)	94.6 (31.9)
Fuel Cell	52.2 (18.3)	96.7 (34.0)

8. CONCLUSION

It has been shown through the experimental portion of this study that volatile methyl siloxanes present in LFG have adverse effects on reforming catalysts when decomposed to silica. Temperature programmed reduction experiments showed that the 6M-Pt catalyst had a reduction temperature of 315 °C which is 67 °C higher than the fresh catalyst which had a reduction temperature of 248 °C. Even at the smallest poisoning amount of 1 week, the reduction temperature increased to 304 °C for the 1W-Pt catalyst. A similar observation was present in the high temperature reforming catalyst which lacks the presence of platinum. The fresh catalyst had a reduction temperature of 382 °C whereas the 6M-NiMg catalyst had a reduction temperature of 546 °C, the 1M-NiMg catalyst had a reduction temperature of 473 °C compared to 407 °C for the 1W-NiMg catalyst. Reaction experiments also indicated that the presence of poisoning caused a reduction in the catalyst activity likely as a result of the silica blocking some of the catalyst pores and/or active sites. This theory is supported by the reduction of surface areas observed through physisorption studies especially for the high temperature reforming catalyst where the fresh catalyst had a high SA of 40m^2/g compared to 1 week poisoning with a surface areas of 35 m^2/g and 28.2 m^2/g for 6 months of poisoning. Both the NiMg and 0.16Pt catalysts showed the same trend of increasing X_{10} as well as X_{50} conversion temperatures for CH_4 and CO_2 with increased poisoning amounts. The fresh 0.16Pt catalyst had a CH_4 X_{10} conversion temperature of 454°C

(Elsayed *et al* 2015) whereas at 1W-Pt the temperature increased to 518.4 °C reaching a high of 586.8 °C for 6M-Pt. Methane X_{50} conversion temperature increased from 603.3 °C for the fresh catalyst to a high of 752.3 °C for the 6M-Pt catalyst where 1W-Pt had an X_{50} of 630.1°C and 675.1 °C for 1M-Pt catalyst. Carbon dioxide X_{10} and X_{50} conversion temperatures increased from 432.0 °C and 578.0 °C for the fresh 0.16Pt catalyst to a high of 565.5 °C and 726.1 °C respectively for the 6M-Pt catalyst.

NiMg only catalysts had a similar increase in reforming temperature where the fresh catalyst had a CH_4 X_{10} conversion temperature of 762.3 °C (Elsayed *et al* 2015) which increased to 809.8 °C for 1W-NiMg sample and 841.8 °C for the 6M-NiMg catalyst. Furthermore, for the NiMg only catalyst, CH_4 did not reach X_{50} at the 1M-NiMg and 6M-NiMg as the maximum tested reaction temperature of 900 °C was reached. Similarly, the CO_2 X_{50} conversion was not attained for the same catalyst (6M- NiMg). However the CO_2 X_{10} temperature increased from 742.4 °C for the fresh NiMg catalyst to 789.7 °C for the 1W-NiMg sample and 826.8 °C for the 1M-NiMg catalyst and reached 900 °C for the 6M-NiMg one.

Although the deposited silica which simulated decomposed VMS had adverse effects in both catalyst systems as already shown, the 0.16Pt catalyst was more resilient compared to the NiMg-only catalyst. This is evident by the results shown that 0.16Pt catalyst had both X_{10} as well as X_{50} conversion for both CH_4 and CO_2 at even the 6M-Pt catalyst (corresponding to a poisoning amount of 6 months). On the other hand, the NiMg only catalyst did not hold as well when poisoned where it lacked CH_4 X_{50} conversion at 1M-NiMg and had no observable CH_4 conversion at all at 6M-NiMg. Furthermore, the CO_2 X_{50} conversion was also not attained at the 6M-NiMg catalyst. Nonetheless, the results of this study have shown that VMS are harmful to the reforming catalysts both low and high temperature ones. The catalyst systems showed signs of deactivation even at low amounts of poisoning as shown. Therefore it is imperative that the LFG be scrubbed from VMS as their presence only causes harm and will increase overall operating costs since both equipment and catalysts will have to be serviced and/or replaced more frequently as a result.

Through the COMSOL® simulation, it was shown that the appropriate size for each applications VMS adsorption beds were 10, 20, and 30 feet, respectively. Each utilized 2 parallel VMS

adsorption beds made from schedule 40 carbon steel piping with a 2 foot outer diameter. These sizes gave respective breakthrough times of 195, 194, and 217 days for VMS.

The cost analysis performed included VMS and H_2S which are both especially harmful contaminants for all LFG utilization routes. The annual costs are; \$1.159E6 per year for engines, \$1.192E6 per year for catalysis, and \$1.217E6 per year for fuel cells. This corresponds to respective costs of \$0.031/Nm^3, \$0.032/Nm^3, and \$0.033/Nm^3 for a volume of gas processed basis and \$31.8/kg, \$32.6/kg, and \$33.3/kg on an amount of contaminant removed basis. The H_2S removal requires more costly equipment and more adsorbent, causing it to be the dominant cost of the entire process. When only VMS is a contaminant, the costs decrease. However, the mass basis costs shoot up to \$820/kg, \$729/kg, and \$768/kg, respectively because dilute contaminants are more costly to remove due to the difference in adsorption behavior (thermodynamics and kinetics) for low concentrations.

No matter if LFG is cleaned and sold or cleaned and used for one of the three energy applications, the economic impact analysis indicates that LFG purification is feasible for all applications, especially when only siloxane removal is necessary. The only case for which it may not be feasible is if both H_2S and siloxanes need to be removed for an engine application. This is a very unlikely scenario since typical H_2S concentrations in LFG are lower than engine sulfur limits.

9. REFERENCES

Ajhar, M., Travesset, M., Yüce, S., and Melin, T. "Siloxane removal from landfill and digester gas – A technology overview," Biores Tech. 101: 2913 (2010).

Álvarez-Flórez, J., and Egusquiza, E. "Analysis of damage caused by siloxanes in stationary reciprocating internal combustion engines operating with landfill gas," Engin Fail Analysis. 50: 29 (2015).

Arnold, M. "Reduction and monitoring of biogas trace compounds," VTT RESEARCH NOTES 2496. (2009).

Bade Shrestha, S.O., and Narayanan, G. "Landfill gas with hydrogen addition – A fuel for SI engines," Fuel. 87: 3616 (2008).

Baudouin, D., Candy, J.-P., Rodemerck, U., Krumeich, F., Veyre, L., Webb, P.B., Thieuleux, C., and Copéret, C. "Preparation of Sn-doped 2–3 nm Ni nanoparticles supported on SiO_2 via surface organometallic chemistry for low temperature dryreforming catalyst: The effect of tin doping on activity,selectivity and stability," Catal Tod. 235: 237 (2014).

Bioenergy, I. "Task 24: Energy from biological conversion of organic waste," http://wwwiea-biogasnet/files/daten-redaktion/download/publi-task37/Biogas%20upgradingpdf.

Boulinguiez, B., and Le Cloirec, P. "Adsorption on Activated Carbons of Five Selected Volatile Organic Compounds Present in Biogas: Comparison of Granular and Fiber Cloth Materials," Energy Fuels. 24: 4756 (2010).

Bradford, M.C.J., and Vannice, M.A. "Catalytic reforming of methane with carbon dioxide over nickel catalysts I. Catalyst characterization and activity," Appl Catal A: Gen. 142: 73 (1996).

Bradford, M.C.J., and Vannice, M.A. "CO_2 Reforming of CH_4," Catal Rev: Sci Engin. 41: 1 (1999).

Cabrera-Codony, A., Montes-Morán, M.A., Sánchez-Polo, M., and Martin, M.A. "Biogas Upgrading: Optimal Activated Carbon Properties for Siloxane Removal," Environ Sci Technol. 48: 7187 (2014).

Cheng, P., Zheng, M., Jin, Y., Huang, Q., and Gu, M. "Preparation and characterization of silica-doped titania photocatalyst through sol–gel method," Mat Lett. 57: 2989 (2003).

Czyrnek-Delêtre, M.M., Ahern, E.P., and Murphy, J.D. "Is small-scale upgrading of landfill gas to biomethane for use as a cellulosic transport biofuel economically viable?," Biofuels, Bioprod Bioref. 10: 139 (2016).

Damyanova, S., Pawelec, B., Arishtirova, K., Fierro, J.L.G., Sener, C., and Dogu, T. "MCM-41 supported PdNi catalysts for dry reforming of methane," Appl Catal B: Environ. 92: 250 (2009a).

Damyanova, S., Pawelec, B., Arishtirova, K., Huerta, M.V.M., and Fierro, J.L.G. "The effect of CeO_2 on the surface and catalytic properties of $Pt/CeO_2–ZrO_2$ catalysts for methane dry reforming," Appl Catal B: Environ. 89: 149 (2009b).

Dantas, S.C., Escritori, J.C., Soares, R.R., and Hori, C.E. "Effect of different promoters on $Ni/CeZrO_2$ catalyst for autothermal reforming and partial oxidation of methane," Chem Engin J. 156: 380 (2010).

de Arespacochaga, N., Valderrama, C., Mesa, C., Bouchy, L., and Cortina, J.L. "Biogas deep clean-up based on adsorption technologies for Solid Oxide Fuel Cell applications," Chem Engin J. 255: 593 (2014).

de Arespacochaga, N., Valderrama, C., Raich-Montiu, J., Crest, M., Mehta, S., and Cortina, J.L. "Understanding the effects of the origin, occurrence, monitoring, control, fate and removal of siloxanes on the energetic valorization of sewage biogas—A review," Ren Sus Energy Rev. 52: 366 (2015).

Dewil, R., Appels, L., and Baeyens, J. "Energy use of biogas hampered by the presence of siloxanes," Energy Conv Manag. 47: 1711 (2006).

Dry, M.E. In: André S, Mark D, eds. Fischer-Tropsch Technology: Studies in Surface Science and Catalysis. USA: Elsevier, 2004:196-257.

Dry, M.E. "The Fischer–Tropsch process: 1950–2000," Catal Tod. 71: (2002).

EERE. Alternative Fuels Data Center: Fuel Prices. 2016 December, 2016 [cited; Available from: http://www.afdc.energy.gov/fuels/prices.html]

EIA "Electric Power Monthly," https://www.eia.gov/electricity/monthly/epm_table_grapher.cfm?t=epmt_5_6_a (2016a).

EIA. Henry Hub Natural Gas Spot Price. 2017 February 1, 2017 [cited; Available from: https://www.eia.gov/dnav/ng/hist/rngwhhdM.htm]

EIA. How much does it cost to generate electricity with different types of power plants? 2016b August 8, 2016 [cited; Available from: http://www.eia.gov/tools/faqs/faq.cfm?id=19&t=3]

EIA "Key world energy statistics," http://www.iea.org/publications/freepublications/publication/KeyWorld2016.pdf (2016c).

Elsayed, N.H., Roberts, N., Joseph, B., and Kuhn, J.N. "Comparison of Pd-Ni-Mg/ceria-zirconia and Pt-Ni-Mg/ceria-zirconia catalysts for syngas production via low temperature reforming of model biogas," Top in Catal. 59: 138 (2016).

Elsayed, N.H., Roberts, N., Joseph, B., and Kuhn, J.N. "Low temperature dry reforming of methane over Pt-Ni-Mg/ceria-zirconia catalysts," Appl Catal B: Environ. 179: 213 (2015).

EPA "Accomplishments of the Landfill Methane Outreach Program," https://www.epa.gov/lmop/accomplishments-landfill-methane-outreach-program (3/28/17) (2016a).

EPA "Landfill Gas Energy Project Development Handbook," Landfill Methane Outreach Program (LMOP). (2016b).

EPA "Methane Emissions," https://www.epa.gov/ghgemissions/overview-greenhouse-gases#methane (3/27/17) (2016c).

EPA "Operation Projects," https://www3epagov/lmop/projects-candidates/operationalhtml. last accessed 8/16/16 (2016d).

Estefanía López, M., Rene, E.R., Veiga, M.C., and Kennes, C. "Biogas Technologies and Cleaning Techniques," Environmental Chemistry for a Sustainable World. 347 (2012).

Finocchio, E., Garuti, G., Baldi, M., and Busca, G. "Decomposition of hexamethylcyclotrisiloxane over solid oxides," Chemosphere. 72: 1659 (2008).

Finocchio, E., Montanari, T., Garuti, G., Pistarino, C., Federici, F., Cugino, M., and Busca, G. "Purification of Biogases from Siloxanes by Adsorption: On the Regenerability of Activated Carbon Sorbents," Energy Fuels. 23: 4156 (2009).

Fogler, H.S. Elements of Chemical Reaction Engineering 4th ed. ed. New York: Pearson, 2006.

Gadde, B. "Economic Utilisation of Biogas as a Renewable Fuel for Fuel Cell," The 2nd Joint International Conference on “Sustainable Energy and Environment (SEE 2006)". 1 (2006).

Geankoplis, C.J. Transport processes and unit operations. 3rd ed: Prentice-Hall International, 1993.

Gebrezgabher, S.A., Meuwissen, M.P.M., Prins, B.A.M., and Oude Lansink, A.G.J.M. "Economic analysis of anaerobic digestion—A case of Green power biogas plant in The Netherlands," NJAS -Wageningen J Life Sci. 57: 109 (2010).

Gislon, P., Galli, S., and Monteleone, G. "Siloxanes removal from biogas by high surface area adsorbents," Waste Manag 33: 2687 (2013).

Haga, K., Adachi, S., Shiratori, Y., Itoh, K., and Sasaki, K. "Poisoning of SOFC anodes by various fuel impurities," Sol Stat Ion. 179: 1427 (2008).

Hepburn, C.A., Martin, B.D., Simms, N., and McAdam, E.J. "Characterization of full-scale carbon contactors for siloxane removal from biogas using online Fourier transform infrared spectroscopy," Environ Tech. 36: 178 (2015).

Herdin, G.R., Gruber, F., Kuffmeier, R., and Brandt, A. "Solutions for Siloxane Problems in Gas Engines Utilizing Landfill and Sewage Gas," ASME Spring Technical Conference. 34-3: (2000).

Hill, A. "Conduct a Nationwide Survey of Biogas Cleanup Technologies and Costs," Final Report. AQMD Contract #: 13432: (2014).

Hokenek, S., Walker, D., Daza, Y.A., Qayyum, E., Yung, M.M., Wolan, J.T., and Kuhn, J.N. "Challenges and Consequences of Carbon Dioxide as an Oxidizing Agent for Hydrogen Generation from Hydrocarbons," Tech Innov. 14: 115 (2012).

Jafari, T., Jiang, T., Zhong, W., Khakpasha, N., Delljoo, B., Aindow, M., Singh, P., and Suib, S.L. "Modified Mesoporous Silica for Efficient Siloxane Capture," Langmuir. 32: 2369 (2016).

Jafari, T., Noshadi, I., Khakpasha, N., and Suib, S.L. "Superhydrophobic and stable mesoporous polymeric adsorbent for siloxane removal: D4 super-adsorbent," J Mater Chem A. 3: 5023 (2015).

Jiang, T., Zhong, W., Jafari, T., Du, S., He, J., Fu, Y.-J., Singh, P., and Suib, S.L. "Siloxane D4 adsorption by mesoporous aluminosilicates," Chem Engin J. 289: 356 (2016).

Kent, R.A. "Conversion of Landfill Gas to Liquid Hydrocarbon Fuels: Design and Feasibility Study," Department of Chemical & Biomedical Engineering. M.S.: (2016).

Kuhn, J.N., Elwell, A.C., Elsayed, N.H., and Joseph, B. "Requirements, techniques, and costs for contaminant removal from landfill gas," Waste Manag. (2017).

Laosiripojana, N., and Assabumrungrat, S. "Methane steam reforming over Ni/Ce–ZrO_2 catalyst: Influences of Ce–ZrO_2 support on reactivity, resistance toward carbon formation, and intrinsic reaction kinetics," Appl Catal A: Gen. 290: 200 (2005).

Madi, H., Diethelm, S., Poitel, S., Ludwig, C., and Van Herle, J. "Damage of Siloxanes onNi-YSZ Anode Supported SOFC Operated on Hydrogen and Bio-Syngas," Fuel Cells. 15: 718 (2015).

Matsui, M., and Imamura, S. "Removal of siloxane from digestion gas of sewage sludge," Biores Techn. 101: S29 (2010).

Mito-oka, Y., Horike, S., Nishitani, Y., Masumori, T., Inukai, M., Hijikata, Y., and Kitagawa, S. "Siloxane D4 capture by hydrophobic microporous materials," J Mater Chem A. 1: 7885 (2013).

Montanari, T., Finocchio, E., Bozzano, I., Garuti, G., Giordano, A., Pistarino, C., and Busca, G. "Purification of landfill biogases from siloxanes by adsorption: A study of silica and 13X zeolite adsorbents on hexamethylcyclotrisiloxane separation," Chem Engin J. 165: 859 (2010).

Mortensen, P.M., and Dybkjær, I. "Industrial scale experience on steam reforming of CO2-rich gas," Appl Catal A: Gen. 495: 141 (2015).

Mota, N., Alvarez-Galvan, C., Navarro, R.M., and Fierro, J.L.G. "Biogas as a source of renewable syngas production: advances and challenges," Biofuels. 2: 325 (2011).

Nam, S., Namkoong, W., Kang, J.-H., Park, J.-K., and Lee, N. "Adsorption characteristics of siloxanes in landfill gas by the adsorption equilibrium test," Waste Manag. 33: 2091 (2013).

NREL "Biomass Energy Basics," http://www.nrel.gov/learning/re_biomass.html, 8/11/2015 (2014).

Oshita, K., Ishihara, Y., Takaoka, M., Takeda, N., Matsumoto, T., Morisawa, S., and Kitayama, A. "Behaviour and adsorptive removal of siloxanes in sewage sludge biogas," Water Sci & Technol. 61: 2003-2012 (2010).

Pakhare, D., and Spivey, J.J. "A review of dry (CO2) reforming of methane over noble metal catalysts," Chem Soc Rev. 43: 7813 (2014).

Papadias, D.D., Ahmed, S., and Kumar, R. "Fuel quality issues with biogas energy - An economic analysis for a stationary fuel cell system," Energy. 44: 257 (2012).

Papurello, D., Lanzini, A., Leone, P., Santarelli, M., and Silvestri, S. "Biogas from the organic fraction of municipal solid waste: Dealing with contaminants for a solid oxide fuel cell energy generator," Waste Manag. 34: 2047 (2014).

Raich-Montiu, J., Ribas-Font, C., de Arespacochaga, N., Roig-Torres, E., Broto-Puig, F., Crest, M., Bouchya, L., and Cortina, J.L. "Analytical methodology for sampling and analysing eight siloxanesand trimethylsilanol in biogas from different wastewater treatmentplants in Europe," Anal Chim Acta. 812: 83 (2014).

Rasmussen, S.B., Kustov, A., Due-Hansen, J., Siret, B., Tabaries, F., and Fehrmann, R. "Characterization and regeneration of Pt-catalysts deactivated in municipal waste flue gas," Appl Catal B: Environ. 69: 10 (2006).

Ribeiro, A.M., Neto, P., and Pinho, C. "Mean Porosity and Pressure Drop Measurements in Packed Beds of Monosized Spheres: Side Wall Effects " Internat Rev Chemical Engin. 2: 40 (2010).

Ricaure-Ortega, D., and Subrenat, A. "Siloxane treatment by adsorption into porous materials," Environ Tech. 30: 1073 (2009).

Rostrup-Nielsen, J.R., Sehested, J., and Norskov, J. "Hydrogen and Synthesis Gas by Steam- and CO2 Reforming," Adv Catal. 47: 65 (2002).

Rucker, C., and Kummerer, K. "Environmental Chemistry of Organosiloxanes," Chem Rev. 115: 466 (2015).

Ruiz, J.A.C., Passos, F.B., Bueno, J.M.C., Souza-Aguiar, E.F., Mattos, L.V., and Noronha, F.B. "Syngas production by autothermal reforming of methane on supported platinum catalysts," Appl Catal A: Gen. 334: 259 (2008).

Ryckebosch, E., Drouillon, M., and Vervaeren, H. "Techniques for transformation of biogas to biomethane," Biomass Bioenergy. 35: 1633-1645 (2011).

Schweigkofler, M., and Niessner, R. "Removal of siloxanes in biogases," J Hazard Mat. B83: 183 (2001).

SEPA "Guidance on gas treatment technologies for landfill gas engines," Environment Agency. (2004).

Sevimoglu, O., and Tansel, B. "Composition and source identification of deposits forming in landfill gas (LFG) engines and effect of activated carbon treatment on deposit composition," J Environ Manag 128: 300 (2013a).

Sevimoglu, O., and Tansel, B. "Effect of persistent trace compounds in landfill gas on engine performance during energy recovery: A case study," Waste Manag. 33: 74 (2013b).

Shiratori, Y., Ijichi, T., Oshima, T., and Sasaki, K. "Internal reforming SOFC running on biogas," Inter J Hydrog Energy. 35: 7905 (2010).

Shiratori, Y., Oshima, T., and Sasaki, K. "Feasibility of direct-biogas SOFC," Inter J Hydrog Energy. 33: 6316 (2008).

Sigot, L., Ducom, G., Benadda, B., and Labouré, C. "Adsorption of octamethylcyclotetrasiloxane on silica gel for biogas purification," Fuel. 135: 205 (2014).

Sigot, L., Ducom, G., Benadda, B., and Labouré, C. "Comparison of adsorbents for H_2S and D4 removal for biogas conversion in a solid oxide fuel cell," Environ Tech. 37: 86 (2016).

Sigot, L., Ducom, G., and Germain, P. "Adsorption of octamethylcyclotetrasiloxane (D4) on silica gel (SG): Retention mechanism," Micro Meso Mat. 213: 118 (2015).

Sinnot, G.T. Chemical Engineering Design. 2nd ed: Elsevier, 2012.

Song, C., and Pan, W. "Tri-reforming of methane: a novel concept for catalytic production of industrially useful synthesis gas with desired H2/CO ratios," Catal Tod. 98: 463 (2004).

Spiegel, R.J., and Preston, J.L. "Technical assessment of fuel cell operation on landfill gas at the Groton, CT, landfill," Energy. 28: 397 (2003).

Staley, B.F. "Trends in Beneficial Use of Landfill Gas & Potential Impacts of Organics Diversion," EREF. LMOP Workshop: https://www3.epa.gov/lmop/documents/pdfs/2016_02_TrendsinBeneficialUseofLandfillGas_BryanStaley_508.pdf, last accessed 8/16/16. (2016).

Sun, Q., Li, H., Yan, J., Liu, L., Yu, Z., and Yu, X. "Selection of appropriate biogas upgrading technology - a review of biogas cleaning, upgrading and utilisation," Ren Sus Energy Rev. 51: 521 (2015).

Surita, S.C., and Tansel, B. "Evaluation of a Full-Scale Water-Based Scrubber for Removing Siloxanes from Digester Gas: A Case Study," Water Environment Research. 87: 444 (2015a).

Surita, S.C., and Tansel, B. "Preliminary investigation to characterize deposits forming during combustion of biogas from anaerobic digesters and landfills," Ren Energy. 80: 674 (2015b).

Tang, X., Misztal, P.W., Nazaroff, W.W., and Goldstein, A.H. "Siloxanes Are the Most Abundant Volatile Organic Compound Emitted from Engineering Students in a Classroom," Environ Sci Technol Lett. 2: (2015).

Tansel, B., and Surita, S.C. "Siloxanes in MSW: Quantities in Waste Components, Release Mechanisms during Waste Decomposition and Fate in the Environment," Hinkley Center for Solid and Hazardous Waste Management. http://www.hinkleycenter.org/images/stories/Tansel_Siloxanes_in_MSW.pdf: (2013).

Urban, W., Lohmann, H., and Salazar Gómez, J.I. "Catalytically upgraded landfill gas as a cost-effective alternative for fuel cells," J Pow Sourc. 193: 359 (2009).

Walker, D.M., Pettit, S., Wolan, J.T., and Kuhn, J.N. "Synthesis Gas Production to Desired Hydrogen to Carbon Monoxide Ratios by Tri-Reforming of Methane Using Ni-MgO-(Ce,Zr)O_2 Catalysts," Appl Catal A: Gen. 445: 61 (2012).

Wheless, E., and Pierce, J. "Siloxanes in Landfill and Digester Gas Update," SWANA Landfill Gas Symposium. http://www.scsengineers.com/scs-white-papers/siloxanes-in-landfill-and-digester-gas-update/ (2004).

Yamaguchi, A., and Iglesia, E. "Catalytic activation and reforming of methane on supported palladium clusters," J Catal. 274: 52 (2010).

Yang, L., Ge, X., Wan, C., Yu, F., and Li, Y. "Progress and perspectives in converting biogas to transportation fuels," Ren Sus Energy Rev. 40: 1133–1152 (2014).

Yoon, S.H. Blower power calculation. 2016 January 27, 2016 [cited; Available from: http://onlinembr.info/cost/blower-power-calculation/

Zhang, Y., Zhang, S., Gossage, J.L., Lou, H.H., and Benson, T.J. "Thermodynamic Analyses of Tri-reforming Reactions To Produce Syngas," Energy Fuels. 28: 2717 (2014).

Zhang, Z., and Verykios, X.E. "Carbon dioxide reforming of methane to synthesis gas over Ni/La_20_3 catalysts," Appl Catal A: Gen. 138: 109 (1996).

Zhang, Z., and Verykios, X.E. "A Stable and Active Nickel-based Catalyst for Carbon Dioxide Reforming of Methane to Synthesis Gas," J Chem Soc, Chem Commun. 71 (1995).